



저작자표시-비영리-변경금지 2.0 대한민국

이용자는 아래의 조건을 따르는 경우에 한하여 자유롭게

- 이 저작물을 복제, 배포, 전송, 전시, 공연 및 방송할 수 있습니다.

다음과 같은 조건을 따라야 합니다:



저작자표시. 귀하는 원저작자를 표시하여야 합니다.



비영리. 귀하는 이 저작물을 영리 목적으로 이용할 수 없습니다.



변경금지. 귀하는 이 저작물을 개작, 변형 또는 가공할 수 없습니다.

- 귀하는, 이 저작물의 재이용이나 배포의 경우, 이 저작물에 적용된 이용허락조건을 명확하게 나타내어야 합니다.
- 저작권자로부터 별도의 허가를 받으면 이러한 조건들은 적용되지 않습니다.

저작권법에 따른 이용자의 권리는 위의 내용에 의하여 영향을 받지 않습니다.

이것은 [이용허락규약\(Legal Code\)](#)을 이해하기 쉽게 요약한 것입니다.

[Disclaimer](#)

**A THESIS
FOR THE DEGREE OF MASTER OF SCIENCE**

**Identification and molecular characterization of two
peroxiredoxin counterparts from Japanese eel**

(*Anguilla japonica*):

Revealing their potent antioxidative properties and putative
immune relevancy



Thantrige Thiunuwan Priyathilaka

**DEPARTMENT OF MARINE LIFE SCIENCES
GRADUATE SCHOOL
JEJU NATIONAL UNIVERSITY
REPUBLIC OF KOREA**

February 2015

**Identification and molecular characterization of two
peroxiredoxin counterparts from Japanese eel
(*Anguilla japonica*): revealing their potent antioxidative
properties and putative immune relevancy**

Thanthrige Thiunuwan Priyathilaka

(Supervised by Professor Jehee Lee)

A thesis submitted in partial fulfillment of the requirement for the degree of

MASTER OF SCIENCE

February 2015

The thesis has been examined and approved by

 제주대학교 중앙도서관

.....
Thesis Director, **Choon Bok Song**, Professor of Marine Life Sciences
School of Bio Medical Sciences, Jeju National University



.....
Bong-Soo Lim, Research Professor
Fish Vaccine Research Center, Jeju National University

.....
Jehee Lee, Professor of Marine Life Sciences
School of Bio Medical Sciences, Jeju National University

Date:.....

**DEPARTMENT OF MARINE LIFE SCIENCES
GRADUATE SCHOOL
JEJU NATIONAL UNIVERSITY
REPUBLIC OF KOREA**

요약문

Peroxiredoxins (Prdx)는 유해한 과산화수소수를 무독한 산물로 감소시킴으로써 세포 산화 스트레스에 중요한 역할을 하는 thiol specific antioxidant enzymes 의 large family 에 속한다. Peroxiredoxin superfamily 는 Prdx1, Prdx2, Prdx3, Prdx4, Prdx5 and Prdx6 라고 알려진 6 개의 isoform 으로 구성되어있다. Prdx 의 6 개는 촉매활성부위에 cysteine residues 의 수에 따라 3 개의 subfamily (typical-2Cys Prdx, atypical-2 Cys Prdx and 1- Cys Prdx) 로 더욱 세분화 된다. Prdxs 사이에서 Prdx4 는 Prdx superfamily 에서 유일하게 분비 단백질인 typical-2Cys Prdx subgroup 에 속한다. Prdx4 는 산화적 스트레스 대응하여 숙주 세포를 보호하거나, 종양 성장의 enhancer 로 작용하고 그리고 신호 전달의 조절과 같은 다양한 범위의 생물학적 과정에서 풍부한 것으로 알려져 있다. One- Cys Pdx subgroup 에 유일하게 포함되어있는 prdx6 isoform 은 possesses peroxidase 와 phospholipase A2 activity 와 같은 두 가지 기능을 가진 세포 내 효소이다. 그러므로 뱀장어(*Anguilla japonica*)와 같은 경제적으로 중요한 수산양식생물 중에서면역학적 측면으로 구조적, 기능적 특성에 대한 Prdx4 와 Prx6 의 역할을 이해하는 것이 중요하다.

이 연구에서는, 이전 cDNA library 를 사용하여 뱀장어(*Anguilla japonica*)에서 Prdx4 와 Prdx6 을 동정하였다. Prdx4 와 Prdx6 의 derived amino acid sequences 는 ClustalW2 multiple sequence alignment 와 EMBOSS needle pairwise sequence alignment 를 사용하여 다른 taxonomic classes 에서 유래한 Prdx4 와 Prdx6 서열을 비교하였다. Orthologous 사이에 관계를 확립하기 위해 계통수 분석은 모든 보고된 Prdx isoforms 를 고려하여 수행되었다. 구조적이고 기능적인 관계를

설명하기 위해서, I-TASSER server 와 PyMOL molecular graphic software 를 사용하여 Prdx4 와 Prdx6 의 컴퓨터 기반 3D 구조적 상동성 모델을 수행하였다. Prdx4 와 Prdx6 의 open reading frame 은 pMAL-c2X expression vector 에 클로닝을 하였다. 그리고 단백질의 항산화적 특성을 결정하기 위해서 정제된 재조합 단백질은 MTT assay 를 하였다. 마지막으로 실시간 PCR(quantitative real time PCR)은 건강한 어류에서 조직 특이적 mRNA 발현과 세균 병원체와 자극제에 의한 유도 후에 전사적인 조절에 대하여 실시하였다.

뱀장어의 Prdx4 (AjPrdx4) 와 Prdx6 (AjPrdx6) 전체 서열은 각각 786bp 와 669bp 이고 262 와 223 아미노산을 암호화하고 있었다. AjPrdx4 의 단백질은 N-terminus (¹¹¹FTFVCPTEI¹²⁰) and C-terminus (²³³GEVCPAGW²⁴⁰) catalytic active sites 을 포함하는 characteristic typical 2-Cys Prdx domain architecture 가 있었다. 반면에, AjPrdx6 은 with N-terminus conserved catalytic active site (PVCTTE)를 가진 1-Cys Prdx sub family 에 속한 domain architecture 와 비슷했다. The AjPrdx4 와 AjPrdx6 모두 *Salmo salar* 와 매우 높은 identity 와 similarity 을 보여주었다. 계통수 분석에서 AjPrdx4 와 AjPrdx6 는 각각 전형적인 2-Cys Prdx ,1-CysPrdx 의 주요 clades 에 속해있었다. AjPrdx4 의 컴퓨터 모의 3D 모델은 핵심에 7 개의 β -sheet 와 측면에 9 개의 α helix 로 구성되어있었다. 반면에, AjPrdx6 는 핵심에 9 개의 β -sheet 와 측면에 7 개의 α -helixes 로 되어있었다. 게다가 앞선 모델들은 기능적인 특성에 대한 AjPrdx4 와 AjPrdx6 의 3D globular arrangement 도 정확한 방향인 것으로 확인되었다.

AjPrdx4 와 AjPrdx6 의 항산화적 특성을 알기 위해서 재조합 단백질을 발현시키고 순수 분리하였다. 재조합 단백질은 산화스트레스와 연계된 H₂O₂ 에

대응하여 뚜렷한 세포 보호 효과를 보여주었다. 산화스트레스에서 AjPrdx4 의 재조합 단백질에서 80% 이상의 cell viability 를 확인하였고 AjPrdx6 의 재조합 단백질에서는 50% 이상의 cell viability 를 관찰하였다. 여기에 우리는 실험한 모든 조직에서 AjPrdx4 와 AjPrdx6 mRNA 전사가 고르게 분포하는 것을 관찰하였다. AjPrdx4 와 AjPrdx6 의 mRNA 전사는 세균(*Edwardsiella tarda*), lipopolysaccharide (LPS) 와 Polyinosinic:polycytidylic (Poly I:C)를 공격 실험하였을 때 간과 비장을 포함한 유력한 면역조직에서 상당히 상향 조절되었다.

종합적으로, 뱀장어의 Prdx4 와 Prdx6 분석한 본 연구는 알려진 Prdx4 와 Prdx6 에서 보존된 전형적인 구조적, 기능적 특성을 보여주었다. 따라서 이 연구는 면역학적 측면에서 뱀장어의 항산화적 특성을 이해하는데 상당한 기여와 가치가 있을 것이다.



SUMMARY

Peroxiredoxins (Prdx) are a large family of thiol specific antioxidant enzymes in eukaryotes and prokaryotes which play a critical role in cellular oxidative stress by reducing harmful peroxide compounds into nontoxic products. The peroxiredoxin superfamily is consisted of six different isoforms, known as Prdx1, Prdx2, Prdx3, Prdx4, Prdx5 and Prdx6. The six members of Prdxs are further categorized into three sub families (typical-2Cys Prdx, atypical-2 Cys Prdx and 1- Cys Prdx) depending on number of cysteine residues present in their catalytic active sites. Among Prdxs the Prdx4 is a member of typical-2Cys Prdx subgroup which is the only a secretory protein in Prdx superfamily. The Prdx4 is known to be involved in plenty of biological process in diverse range, such as protect the host cells against the oxidative stress, and act as an enhancer of tumor growth and regulation of signal transduction. One- Cys Prdx subgroup contains only Prdx6 isoform, is an intracellular bi-functional enzyme which possesses peroxidase and phospholipase A2 activity. Hence, it is important to understand the role of Prdx4 and Prdx6 in economically important aquaculture fish species like Japanese eel (*Anguilla japonica*) with respect to its structural and functional properties in immunological prospective.

In this study, Prdx4 and Prdx6 genes were identified from Japanese eel (*Anguilla japonica*) using previously constructed cDNA library. Derived amino acid sequences of Prdx4 and Prdx6 from Japanese eel were compared with known Prdx4 and Prdx6 sequences from different taxonomic classes using ClustalW2 multiple sequence alignment and EMBOSS needle pairwise sequence alignment. The phylogenetic trees were constructed considering all reported Prdx isoforms in order to establish the relationship between orthologous. In order to elucidate the structural and functional relationship, computer based 3D structural homology models of Prdx4 and

Prdx6 were performed using I-TASSER server and PyMOL molecular graphic software. The open reading frames of both Prdx4 and Prdx6 were cloned into pMAL-c2X expression vector and the purified recombinant proteins were subjected to MTT assay to determine the antioxidant properties of each protein. Finally quantitative real time PCR was performed to examine the tissue specific mRNA expression of these peroxiredoxins in healthy fish and their transcriptional modulation after induction of fish with chemical stimulants and a live bacterial pathogen.

The full length coding sequences of *Anguilla japonica* Prdx4 (*AjPrdx4*) and Prdx6 (*AjPrdx6*) were 786 bp and 669 bp in length which encodes for a 262 and 223 amino acid polypeptides, respectively. The protein of *AjPrdx4* exhibited characteristic typical 2-Cys Prdx domain architecture including N-terminus (¹¹¹FTFVCPTEI¹²⁰) and C-terminus (²³³GEVCPAGW²⁴⁰) catalytic active sites, whereas *AjPrdx6* resembled the domain architecture belonging to the 1-Cys Prdx sub family with N-terminus conserved catalytic active site (⁴⁴PVCTTE⁴⁹). The *AjPrdx4* and *AjPrdx6* exhibited highest amino acids identity and similarity to that of *Salmo salar*. Phylogenetic analysis indicated clustering of *AjPrdx4* and *AjPrdx6* in the main clades of typical 2-Cys Prdx and 1-Cys Prdx respectively. The computer simulated 3D modal of *AjPrdx4* composed of seven core stranded β sheets flanked by nine α helixes, whereas *AjPrdx6* consisted of nine core stranded β -sheets and seven α -helixes. Furthermore generated models affirm that correct orientation of the 3D globular arrangements of *AjPrdx4* and *AjPrdx6* with respect to their functional properties.

In order to characterize the antioxidant properties of *AjPrdx4* and *AjPrdx6* recombinant proteins were expressed and purified. The recombinant proteins showed remarkable cell protection against H₂O₂ mediated oxidative stress. Over 80% of cell viability was detected with recombinant *AjPrdx4*, while over 50% cell viability was

observed with recombinant AjPrdx6 under oxidative stress. Herein we observed ubiquitous distribution of *AjPrdx4* and *AjPrdx6* mRNA transcripts in all the tested tissues. The mRNA transcripts of *AjPRdx4* and *AjPRdx6* were significantly up-regulated in potent immune tissues including liver and spleen upon immune challenge with live bacteria (*Edwardsiella tarda*), lipopolysaccharide (LPS) and Polyinosinic:polycytidylic (Poly I:C).

Collectively, the present study in analysis of Prdx4 and Prdx6 in Japanese eel demonstrated common structural and functional features were conserved with known Prdx4 and Prdx6 counterparts. Hence this study will be valuable and make significant contribution to understand the antioxidant properties of Japanese eel in immunological prospective.



CONTENT

요약문	i
SUMMARY	iv
LIST OF FIGURES	x
LIST OF TABLES	xii
ABBREVIATIONS	xiii
1. INTRODUCTION	1
2. MATERIALS AND METHODS	9
2.1. Identification of <i>AjPrdx4</i> and <i>AjPrdx6</i> cDNA sequences	9
2.2. <i>insilico</i> analysis	9
2.3. Experimental animals	10
2.4. Tissue collection	10
2.5. Immune challenge experiment	10
2.6. RNA extraction	11
2.7. <i>AjPrdx4</i> and <i>AjPrdx6</i> mRNA expression analysis by quantitative real time Polymerase Chain Reaction (qPCR)	12
2.8. Cloning of <i>AjPrdx4</i> and <i>AjPrdx6</i> coding sequences	13
2.9. Overexpression and purification of recombinant <i>AjPrdx4</i> and <i>AjPrdx6</i>	14
2.10. Cell cultures	15

2.11	Protective effects of recombinant AjPrdx4/ AjPrdx6 on cultured cells under oxidative stress	15
3.	RESULTS AND DISCUSSION	17
3.1.	PART 1	17
3.1.1	Sequence characterization	17
3.1.2.	Phylogenetic analysis	21
3.1.3.	Predicted 3D homology modal of AjPrdx6	22
3.1.4.	Tissue distribution analysis of <i>AjPrdx6</i>	25
3.1.5.	Expression profile of <i>AjPrdx6</i> upon <i>E. tarda</i> , LPS and Poly I:C challenge	26
3.1.6.	Over expression and purification of recombinant AjPrdx6	34
3.1.7.	Protective effects of recombinant AjPrdx6 (rAjPrdx6) on cultured cells under oxidative stress	34
3.2.	PART-2	37
3.2.1.	Sequence characterization	37
3.2.2.	Phylogenetic analysis	41
3.2.3.	Modeled tertiary structure of AjPrdx4	42
3.2.4.	Tissue distribution analysis of <i>AjPrdx4</i>	45
3.2.5.	Regulation of <i>AjPrdx4</i> expression in response to pathogenic infection	46
3.2.6.	Over expression of recombinant AjPrdx4 (rAjPrdx4)	51

3.2.7. Protective effects of recombinant rAjPrdx4 on cultured cells under oxidative stress	52
CONCLUSIONS	55
REFERENCES	56
ACKNOWLEDGEMENT	60



LIST OF FIGURES

- Figure 1: Schematic representation of typical 2-Cys peroxiredoxins
- Figure 2: The catalytic cycle of typical 2-Cys Prdx (Prdx4)
- Figure 3: Schematic representation of 1-Cys peroxiredoxin (Prdx6)
- Figure 4: The Japanese eel (*Anguilla japonica*)
- Figure 5: The nucleotide and deduced amino acid sequences of Japanese eel, *Anguilla japonica* Prdx6
- Figure 6: Multiple sequence alignment of different vertebrate Prdx6s
- Figure 7: Phylogenetic tree of known Prdxs from different species including the AjPrdx6
- Figure 8A: Computer simulation model generated for the AjPrdx6
- Figure 8B: 3D structure of AjPrdx6 with important conserved amino acid residues
- Figure 9: Tissue specific expression analysis of *AjPrdx6* mRNA in healthy *Anguilla japonica* by qPCR
- Figure 10A,B: Relative mRNA expression pattern of *AjPrdx6* in liver after the stimulation with *Edwardsiella tarda* (A) and LPS (B)
- Figure 10C: Relative mRNA expression pattern of *AjPrdx6* in liver after the stimulation with Poly I:C
- Figure 11A,B: Relative mRNA expression pattern of *AjPrdx6* in spleen after the stimulation with *Edwardsiella tarda* (A) and LPS (B)
- Figure 11C: Relative mRNA expression pattern of *AjPrdx6* in spleen after the stimulation with Poly I:C (C)
- Figure 12: SDS-PAGE analysis of the rAjPrdx6 fusion protein in *E. coli* BL21
- Figure 13: Effects of recombinant AjPrdx6 on cell growth and viability
- Figure 14: The nucleotide and deduced amino acid sequences of Japanese eel, *Anguilla japonica* Prdx4
- Figure 15: Multiple sequence alignment of different vertebrate Prdx4s
- Figure 16: Phylogenetic tree of known Prdxs from different species including the AjPrdx4

- Figure 17A: Computer simulation model generated for the AjPrdx4
- Figure 17B: The 3D structure of AjPrdx4 with important conserved amino acid residues
- Figure 18: Tissue specific expression analysis of AjPrdx4 mRNA in healthy *Anguilla japonica* by qPCR
- Figure 19A: Relative mRNA expression pattern of AjPrdx4 in liver after the stimulation with *Edwardsiella tarda*
- Figure 19B,C: Relative mRNA expression pattern of AjPrdx4 in liver after the stimulation with LPS (B) and Poly I:C (C)
- Figure 20: SDS-PAGE analysis of the rAjPrdx4 fusion protein in E. coli BL21
- Figure 21A: Effects of recombinant AjPrdx4 on cell growth and viability
- Figure 21B,C: Microscopic image of vero cells after the H₂O₂ (B), Microscopic image of rAjPrdx4 (50µg/mL) pretreated vero cells with DTT (1 mM) followed by H₂O₂ (500 µM) (c)



LIST OF TABLES

- Table 1.** Oligomers used in this study
- Table 2.** Pairwise identity and similarity percentages of AjPrdx6 with selected orthologs at amino acid level
- Table 3.** Pairwise identity and similarity percentages of AjPrdx4 with selected orthologs at amino acid level



ABBREVIATIONS

°C	Degrees of calculus
μL	Microliter
μmol	Micromolar
3D	Three dimensions
<i>AjEF1-a</i>	<i>Anguilla japonica</i> Elongation factor 1 alpha
<i>AjPrdx4</i>	<i>Anguilla japonica</i> peroxiredoxin 4 at protein level
<i>AjPrdx4</i>	<i>Anguilla japonica</i> peroxiredoxin 4 at transcriptional level
<i>AjPrdx6</i>	<i>Anguilla japonica</i> peroxiredoxin 6 at protein level
<i>AjPrdx6</i>	<i>Anguilla japonica</i> peroxiredoxin 6 at transcriptional level
ANOVA	Analysis of variance
BHI	Brain heart infusion
BLAST	Basic local alignment search tool
Bp	Base pair
cDNA	complementary deoxyribonucleic acid
CFU	Colony Forming Unit
CysR-SH	Resolving cysteine
Cys-SOH	Cysteine sulfonic acid
Cys-SpH	Peroxidatic cysteine
DMEM	Dulbecco's Modified Eagle's medium
DNA	Deoxyribonucleic acid
dNTP	Deoxynucleotide-triphosphate
DTT	Dithiothreitol
<i>E.tarda</i>	<i>Edwardsiella tarda</i>
FAO	Food and Agriculture Organization of the United Nations
FBS	Fetal bovine serum
g	Gram
GSH	Glutathione
h	Hours
IFN	Interferon
IPTG	Isopropyl-β-thiogalactopyranoside
kDa	Kilo Dalton
L	Liter
LB	Luria-Bertani
LPS	lipopolysaccharide
MBP	Maltose binding protein
MEGA	Molecular Evolutionary Genetic Analysis
mg	Milligram
min	Minute(s)
mM	Milimolor
mRNA	Messenger ribonucleic acid
MTT	3-(4, 5-dimethyl-thiazol-2-yl) 2, 5-diphenyltetrazolium bromide

NADPH	Nicotinamide adenine dinucleotide phosphate
NJ	Neighbor joining
NKFE	Natural killer enhancing factor
Nm	Nanometer(s)
OD	Optical density
ORF	Open Reading Frame
p.i.	Post injection
PAMPs	Pathogen associated molecular patterns
PBS	Phosphate buffered saline
PCR	Polymerase chain reaction
PI	Iso electric point
PLA2	Phospholipase A2
Pmol	Picomolar
Poly IC	Polyinosinic:polycytidylic
Prdx	Peroxiredoxin
PRR	Pattern recognition receptor
qPCR	Quantitative Real time polymerase chain reaction
rAjPrdx4	Recombinant <i>Anguilla japonica</i> peroxiredoxin 4
rAjPrdx6	Recombinant <i>Anguilla japonica</i> peroxiredoxin 6
RCSB	Research Collaboratory for Structural Bioinformatics
RNA	Ribonucleic acid
U	units
ROS	Reactive Oxygen Species
rpm	Revolutions per minutes
SDS-PAGE	Sodium dodecyl sulfate Polyacrylamide gel electrophoresis
SE	Standard error
SMART	Simple Modular Architecture Research Tool
SOD	Superoxide dismutase
TLR	Toll like receptor
WSSV	White spot syndrome virus

1. INTRODUCTION

Oxidative stress and antioxidants

Reactive oxygen species (ROS) are chemically reactive oxygen containing molecules, which are synthesized by aerobic organisms as a byproduct of aerobic respiration. Superoxides, hydrogen peroxides, hydroxyl radicals and nitric oxides are well known physiologically important ROS involved in several beneficial and adverse effects to organisms (Nordberg and Arner, 2001). Minor concentrations of this ROS are mandatory for the normal cellular functions, such as intracellular signal transduction, regulation of gene expression, intracellular redox regulation and etc. (Palmer et al., 1987; Furchgott, 1995). Moreover ROS play a significant role in host defense against pathogenic infections (Thomas et al., 1988). Upon the pathogenic attack, subsequently activated phagocytes can produce adequate level of ROS under catalysis of myeloperoxidase, NADPH oxidase like enzymes for counterattack the pathogenic invasion in host organism (Rosen et al., 1990). Among this highly reactive ROS (hypochlorous acid, hydroxyl radicals), which are produced in phagosomes elicit their extreme bactericidal activity by destruction of DNA replication in invading microorganisms (Rosen et al., 1990). However excessive production of ROS leads to accumulation of free oxygen intermediates in intracellular environment is referred to as oxidative stress. Several deleterious physiological impairments of oxidative stress are being reported under different categories including nucleic acid damage, protein oxidation, lipid peroxidation, modification of lipoproteins involved in atherosclerosis and apoptosis (Yla-Herttuala, 1999; Stadtman and Levine, 2000; Nordberg and Arner, 2001). Hence maintenance of optimum intracellular ROS level is vital for regulation of typical cellular functions.

Antioxidants are known to play a critical role in intracellular ROS level balancing, which can detoxify deleterious oxygen intermediates without disrupting normal cellular functions. To date, several types of enzymatic and non-enzymatic antioxidants have been identified in living organisms (Nordberg and Arner, 2001). Catalases, Superoxide dismutase (SOD), peroxiredoxins, glutathione (GSH), glutaredoxines, glutathione peroxidases, thioredoxines and superoxide reductase are few examples for cellular enzymatic antioxidant system, while vitamin C and E, selenium compounds, lipoic acid have been categorized as non-enzymatic antioxidants (Rudneva, 1999; Nordberg and Arner, 2001).

Peroxiredoxins and their mechanism of action during the oxidative stress

Peroxiredoxins (Prdxs) are a large family of thiol peroxidases, which play a pivotal role in cellular oxidative stress by reducing the hydrogen peroxide, peroxynitrite and various kinds of organic hydroperoxides into nontoxic form (Wood et al., 2003; Kawazu et al., 2008). Typically Prdxs can be identified in all kingdoms of life including plants, animals and yeasts (Wood et al., 2003). Recently six different isoforms of Prdxs (Prdx1-Prdx6) which are encoded by multiple genes have been discovered in mammals (Perez-Sanchez et al., 2011). The six members of the Prdx family further divided into three major subgroups depending on the number and position of catalytic cysteine (Cys) residue, which is also referred to as the peroxidatic cysteine (Cys-SpH) (Ellis and Poole, 1997a; Ellis and Poole, 1997b; Chae et al., 1999; Wood et al., 2003). Typical 2-Cys Prdxs, atypical 2-Cys Prdxs and the 1-Cys Prdxs are three major classes of Prdxs, among them typical 2-Cys Prdx subgroup (Prdx1-Prdx4) is considered as the largest subgroup, which contains conserved N terminus Cys residue (peroxidatic cysteine) and the conserved C terminus resolving Cys residue (CySR-SH) (Chae et al., 1999; Wood et al., 2003; Kawazu et al., 2008; Aran et al., 2009). The Prdx5 belongs to the atypical

2-Cys Prdx subgroup which contains only N terminus Cys residue and non –conserved Cys residue for acquire its activity, whereas the 1-Cys Prdx subgroup (Prdx6) comprises only with conserved peroxidatic cysteine residue at the N terminus (Choi et al., 1998; Chae et al., 1999; Rhee et al., 2001; Wood et al., 2003).

Basically, the catalytic reaction of all three Prdx subgroups is divided into two steps (Wood et al., 2003). During the first step of peroxidase reaction mechanism in all three Prdx subgroups, the peroxidatic cysteine (Cys-SpH) is oxidized into cysteine sulfonic acid (Cys-SOH) after attacking to the peroxide substrates (Ellis and Poole, 1997a; Ellis and Poole, 1997b). However, second step of the peroxidase mechanism of each Prdx class has remarkable characteristic properties. The C-terminus resolving Cys residue (CySR-SH) of typical 2-Cys Prdx subgroup is attacked by oxidized N-terminus Cys residue in different Prdx molecule (Cys-SOH) and subsequently forms an intermolecular disulfide bond (Kawazu et al., 2008), whereas the atypical 2-Cys Prdx class forms an intramolecular disulfide bridge (Chae et al., 1999; Wood et al., 2003). Finally, reduction of the disulfide bonds and regeneration of reduced state of the peroxidatic cysteine (Cys-SpH) is occurred by the action of thiol containing enzymes like thioredoxins, tryparedoxin, glutaredoxin and glutathione (Nogoceke et al., 1997; Poole et al., 2000; Bryk et al., 2002; Sutton et al., 2010). Reduction of the cysteine sulfonic (Cys-SOH) in 1-Cys Prdx subfamily happens similar manner to that of typical 2-Cys and atypical 2-Cys Prdx classes, however the exact redox partner that required for this process has not been verified yet (Peshenko and Shichi, 2001; Hofmann et al., 2002).

Peroxiredoxin 4 (Prdx4)

The Prdx4 is the only secretory protein among the Prdx superfamily, which is secreted through the golgi apparatus (Matsumoto et al., 1999; Sutton et al., 2010). Previous experiments demonstrated that the existence of two different types of Prdx4 in several tissues, that are differ from each other by presence or absence of the N terminal signal sequence (Elofsson and von Heijne, 2007; Giguere et al., 2007). The Prdx4 is known to be involved in plenty of biological process in diverse range, such as protection of host cells against the oxidative stress, act as an enhancer of tumor growth (Lehtonen et al., 2004), spermatogenic process (Giguere et al., 2007; Iuchi et al., 2009), regulation of cellular signal transduction mechanisms involve in innate immunity (Giguere et al., 2007; Palande et al., 2011).

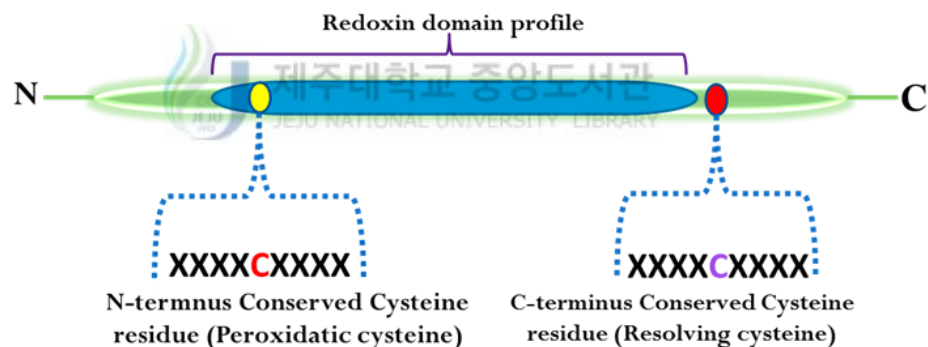


Fig.1. Schematic representation of typical 2-Cys peroxiredoxin. N-terminus and C-terminus of the protein are represented as N and C, respectively. The N-terminus conserved cysteine residue (peroxidatic cysteine) is indicated as yellow circle, whereas C-terminus conserved cysteine residue is depicted as red circle.

This Prdx isoform contains an additional conserved cysteine in the carboxyl-terminal region, thereby categorized into typical 2-Cys Prdx subgroup (Rhee et al., 2005). Typical domain architecture of Prdx4 bears a characteristic redoxin domain profile, catalytic active sites at both N and C terminus along with the conserved peroxidatic and resolving cysteine residues respectively (Fig.1.) (Rhee et al., 2005; Aran et al., 2009). Typically Prdx4 is tending to form a homodimers during the catalytic

cycle and the redox-sensitive cysteine residue of each subunit of the Prdx homodimer is oxidized by H_2O_2 to Cys-SOH, which then reacts with a neighboring CysR-SH of the other subunit to form an intermolecular disulfide (Fig.2.) (Kang et al., 2005; Aran et al., 2009). Finally disulfide bond is reduced by another redox partner for regenerate the reduced form of peroxidatic cysteine. The Prdx4 has recently been discovered and characterized from *Miichthys miiuy* (Ren et al., 2014), *Fenneropenaeus chinensis* (Zhang et al., 2014), *Marsupenaeus japonicus* (Chen et al., 2013) and *Seriola lalandi* (Loo and Schuller, 2010).

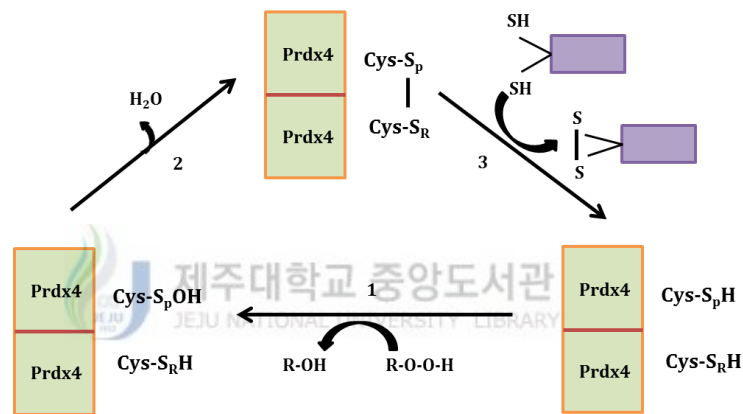


Fig.2. The catalytic cycle of typical 2-Cys Prdx (Prdx4). The peroxide substrate oxidizes the peroxidatic cysteine (Cys-S_pH) to the sulfonic acid form (Cys-S_pOH) (reaction 1) which after reacting with the reduced resolving cysteine residue (Cys-S_RH) of another typical 2-Cys Prdx molecule, yields the homodimer linked via a disulfide bond (reaction 2). Subsequently, the reduced form of redox partner (thioredoxin or glutathione) closes the catalytic cycle, returning the oxidized typical 2-Cys Prdx to reduced state (reaction 3).

Peroxiredoxin 6 (Prdx6)

Prdx6 is a 1-Cys peroxiredoxin family member also called a bifunctional enzyme on the account that it possesses both glutathione-peroxidase activity and phospholipase A2 (PLA2) activity. Typical domain architecture of Prdx6 bears characteristic structural features of 1-Cys Prdxs including redoxin domain profile, active site for phospholipase A2 activity and the N- terminus catalytic active site with

conserved peroxidatic cysteine residue (Fig.3) (Manevich and Fisher, 2005). The prdx6 is identified only in cytosolic environments. During the catalytic cycle, the N-terminus conserved peroxidatic cysteine residue (Cys-SpH) is oxidized into cysteine sulfonic acid. Meanwhile, peroxide substrates (H_2O_2 , organic hydroperoxides) are reduced in to non-toxic forms (H_2O , alcohol). However, due to the absence of C-terminus conserved resolving cysteine residue, resulted cysteine sulfonic acid could not be able to form an intermolecular disulfide bonds like typical 2-Cys Prdxs (Choi et al., 1998; Kang et al., 1998).

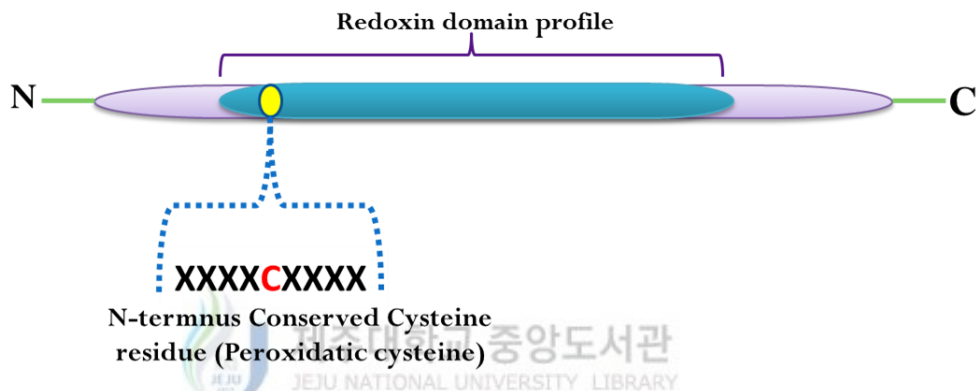


Fig.3. Schematic representation of 1-Cys peroxiredoxin (Prdx6). N-terminus and C-terminus of the protein are represented as N and C, respectively. The N-terminus conserved cysteine residue (peroxidatic cysteine) is indicated as yellow circle.

The Prdx6 may also participate in the activation of neutrophil NADPH oxidase through an interaction with $p67^{phox}$ (Leavey et al., 2002), preventing methemoglobin formation in erythrocyte hemolysates (Stuhlmeier et al., 2003) In plants, they play a role in the determination of seed germination (Haslekas et al., 2003). Recently, Prdx6 has been cloned from several vertebrates and invertebrates, including human (*Homo sapiens*) (Chae et al., 1994), rat (*Rattus norvegicus*) (Fujii et al., 2001), cattle (*Bos taurus*) (Singh and Shichi, 1998), chicken (*Gallus gallus*) (Han et al., 2005), channel catfish (*Ictalurus punctatus*) Chinese mitten crab (*Eriocheir sinensis*) (Mu et al., 2009) and annelid worm (*Arenicola marina*) (Loumaye et al., 2008) and their cDNA

sequences have been characterized. An increasing number of studies have provided evidence that Prdx6 can function *in vivo* as an antioxidant enzyme.

Japanese eel (*Anguilla japonica*)

Recently, fifteen eel species have been identified in all over the world; those belong to the genus *Anguilla* and family of Anguillidae. The Japanese eel (*Anguilla Japonica*) (Fig. 4) is distributed in East Asia including Japan, Taiwan, Eastern China, Korea and Vietnam (Kimura et al. 1994). This fish species have catadromus life cycle spending a part of their life cycle in the fresh water and the spawn stage in the sea. At maturity, the eel migrates from its diverse habitats to a marine spawning site around seamounts west of the Mariana Islands. The eel larvae also refer to as leptocephali are migrated using the North Equatorial current and Kuroshio Current generated from the ground to the continental shelf of East Asian region (Tsukamoto, 1992). Thereafter, leptocephali change their morphology into glass eel and become elvers in estuaries. Then the elvers grow as yellow eels for 4-10 years and another morphological change happen. This stage is known as silver eel stage and, those silver eels migrate back to their birth place to spawn and die (Tzeng et al., 2000)



Fig.4. The Japanese eel (*Anguilla japonica*)

Important of the Japanese eels in aquaculture industry

The Japanese eel (*Anguilla Japonica*) is a one of the most commercially important aquaculture fish species in Japan and Korea, which is considered as high priced fish in market. Total production of Japanese eel in Japan is 30,000 tons and they 80,000 tons of them are imported by China, Taiwan and other countries annually (Hirohiko K. 2006). According to the data of Food and Agriculture Organization (FAO) 2014, within last 60 years Global capture production of Japanese eel is decreased annually and the Global aquaculture production is annually increased. Pathogenic infections are one of the major reasons for the significant mortalities occur in Japanese eel aquaculture industry. Therefore, Japanese eel aquaculture industry has been suffering a tremendous economic loss. Thus, extensive investigation of the Japanese eel immune system is important to improve and facilitate the disease management strategies and to facilitate the long-term sustainability of the aquaculture industry.

Hence, this study has been focused on the molecular characterization of the two peroxiredoxin counterparts (peroxiredoxin 4 and peroxiredoxin 6) from the Japanese eel to investigate their role at protein level. Furthermore, we sought to understand its role in innate immune responses, by analyzing the temporal mRNA expression after under different pathogenic stress conditions.

2. MATERIALS AND METHODS

2.1. Identification of *AjPrdx4* and *AjPrdx6* cDNA sequences

The full length cDNA sequence of *AjPrdx4* and *AjPrdx6* with highest homology to known Prdx4 and Prdx6 were identified using the Basic Local Alignment Search Tool (BLAST;<http://blast.ncbi.nlm.nih.gov/>) from a previously constructed *Anguilla japonica* transcriptomic database by GL-FLX titanium DNA sequencing technology (Roche 454 genome sequencer FLX systems; Macrogen, Republic of Korea).

2.2 *insilico* analysis

The putative open reading frames (ORF) and deduced amino acid sequences along with several physiochemical properties of *AjPrdx4* and *AjPrdx6* were determined using UGENE software (Okonechnikov et al., 2012) and ExPASy ProtParam online tool (<http://web.expasy.org/protparam/>). The anticipated domain structures of *AjPrdx4* and *AjPrdx6* protein were determined by the Simple Modular Architecture Research Tool (SMART) (<http://smart.embl-heidelberg.de>). ClustalW2 (<http://www.ebi.ac.uk/Tools/msa/clustalw2/>) and EMBOSS Needle (http://www.ebi.ac.uk/Tools/psa/emboss_needle/) online servers were used to perform the multiple sequence alignment and pairwise sequence alignment respectively. Phylogenetic trees were reconstructed by the neighbor joining (NJ) method using Molecular Evolutionary Genetic Analysis (MEGA) software version 5.0, validated by 1000 bootstrap replications. Furthermore, 3D structural homology models of *AjPrdx4* and *AjPrdx6* were predicted by ITASSER online server and visualized using PyMOL software.

2.3 Experimental animals

Healthy Japanese eels (*Anguilla japonica*), body weight around 100 g were kept in 400 L tanks with aerated fresh water at a temperature of $24 \pm 1^\circ\text{C}$ in the Marine Sciences Institute of Jeju National University, Republic of Korea. Three weeks prior to the experiment all the Japanese eels were acclimatized to the laboratory conditions.

2.4 Tissue collection

In order to determine the tissue specific expression of *AjPrdx4* and *AjPrdx6*, brain, liver, kidney, head kidney, spleen, heart, gills, intestine, skin, muscles and gonad were isolated from five healthy animals. All the tissues were snap frozen in liquid nitrogen and subsequently stored at -80°C until RNA extraction.

2.5 Immune challenge experiment

In order to determine the temporal mRNA expression of *AjPrdx4* and *AjPrdx6*, four groups of healthy Japanese eels were subjected to the time course immune challenge experiments. For pathogen derived mitogen challenge experiment, 100 μL of lipopolysaccharide (LPS) suspended in phosphate buffered saline (PBS) ($2 \mu\text{g}/\mu\text{L}$; *Escherichia coli* 055:B5, Sigma) and 100 μL of Polyinosinic:polycytidylic (Poly I:C) acid in PBS ($2 \mu\text{g}/\mu\text{L}$, Sigma) were intraperitoneally injected to the each fish from two separate fish groups respectively. The Gram negative bacterial pathogen; *Edwardsiella tarda* was inoculated to the 100 mL of brain heart infusion (BHI) broth supplemented with 1% sodium chloride and incubated in shaking incubator for 10 h at 25°C . Thereafter bacterial cells were harvested by centrifugation at 3000 rpm for 30 min at 4°C . Harvested cells were subsequently resuspended in PBS, and then diluted to desired concentration. Then each fish from another Japanese eel group was subjected to the

intraperitoneal injection of 100 μ L of *E. tarda* in PBS (1×10^7 CFU/ mL). For control group, 100 μ L of PBS was intraperitoneally injected. Fish were sacrificed at 3 h, 6 h, 12 h, 24 h, 48 h and 72 h post injection periods and liver and spleen samples were collected as described in section 2.4.

2.6 RNA extraction

Total RNA was extracted from collected tissues (section 2.4 and 2.5) using TaKaRa RNAiso plus Total RNA extraction reagent according to the manufactures instruction. Extracted RNA was subjected to the DNase treatment (Promega, USA) following the manufactures instructions. Briefly, a 10 μ L reaction was carried out with 8 μ L of extracted RNA, 1 μ L of RQ1 RNase-free DNase (1U) and 1 μ L of RQ1 RNase-free DNase 10 \times reaction buffer. Mixture was incubated at 37 $^{\circ}$ C for 30 min. After incubation, 1 μ L of RQ1 DNase stop solution was added to terminate the reaction and reaction mixture was subsequently incubated at 65 $^{\circ}$ C for 10 min. Concentration at 260 nm and absorbance ratio (260/280) of extracted RNA was determined before and after the DNase treatment using Nanodrop 2000C spectrophotometer (Thermo Scientific, USA). Moreover, 1 μ L of each RNA sample (before and after the DNase treatment) was analyzed on 1% agarose gel stained with ethidium bromide and rest of the samples were stored at -80 $^{\circ}$ C until use in further analysis. Simultaneously working RNA stock for qPCR experiment was prepared by diluting each sample with nuclease free water and stored at -80 $^{\circ}$ C.

2.7 *AjPrdx4* and *AjPrdx6* mRNA expression analysis by quantitative real time Polymerase Chain Reaction (qPCR)

In order to determine the relative mRNA expression of *AjPrdx4* and *AjPrdx6*, qPCR experiment was performed using the TaKaRa TP850 Thermal Cycler Dice™ Real Time System (TaKaRa, Japan). The qPCR experiment for both *AjPrdx4* and *AjPrdx6* was executed using TOPreal™ One-step RT qPCR kit (SYBR Green) (Enzymomics) according to the manufactures instruction with minor modifications, briefly, the qPCR was carried out in 15 µL total reaction mixture containing, 5.75 µL of template RNA (20 ng) in nuclease free water, 0.75 µL of TOPreal™ One-step RT qPCR Enzyme MIX, 7.5 µL of 2× TOPreal™ One-step RT qPCR Reaction MIX and 0.5 µL of each primers (10 pmol/µL) (Table 1). The qPCR thermal profile as follows, hold at 50°C for 30 min, initial denaturation at 95°C for 10 min, 45 cycles of 95°C for 5 sec, 60°C for 10 sec, 72°C for 30 sec, and a single cycle of 95°C 15 sec, 60°C 30 sec and 95°C 15 sec. The *Anguilla japonica* Elongation Factor 1-Alpha (*AjEF1-a*) (GenBank accession no: AB593812) was amplified as an internal control gene using the same qPCR thermal profile. In order to determine the qPCR specificity, the dissociation curves were analyzed, thereafter relative mRNA expression of the *AjPrdx4* and *AjPrdx6* were determined according to the Livak ($2^{-\Delta\Delta CT}$) method (Livak and Schmittgen, 2001). Fold difference of each gene was calculated relative to the un-injected control group (0 h). All the data were collected from five individual samples and presented as mean standard error (SE) of five replicates (n=5). To determine the statistical significance between the experimental and control groups, all the mRNA expression analysis data were subjected to either Student's t-test or one-way analysis of variance (ANOVA) in SPSS 16.0 for Windows. Differences were considered statistically significant at $p < 0.05$.

2.8 Cloning of *AjPrdx4* and *AjPrdx6* coding sequences

The ORFs of *AjPrdx4* and *AjPrdx6* were amplified using target specific primers with the restriction sites of *EcoRI* and *HindIII* (Table 1). The cDNA was synthesized from total RNA that extracted from Japanese eel's liver tissues using Maxime RT PreMix Kit (iNtRON BIOTECHNOLOGY) according to the manufactures instruction. The Polymerase Chain Reaction (PCR) was performed in TaKaRa thermal cycler Dice™ Touch. Briefly, a 50 µL reaction was carried out with 5 µL of template cDNA, 5 µL of 10×PCR buffer, 4 µL of dNTP mixture (2.5 mM each), 2µL of each forward and reverse primer (10 pmol of each), 0.5 µL of T&I™ Prime Taq Polymerase (5 Units/µL) (Tech & Innovation, Korea) and nuclease free water. The PCR thermal profile was, initial denaturation at 95 °C for 3 min, 35 cycles of 95°C for 30 sec, 55°C for 30 sec, 72°C for 1 min and final extension at 72°C for 3 min. Thereafter, each purified PCR product was digested with *EcoRI* and *HindIII* along with the pMAL-c2X vector according to the manufactures instructions. Then the each digested PCR product was analyzed in the 1% agarose gel and excised. Thereafter, desired products were purified and subsequently ligated in to the pMAL-c2X vector. The recombinant pMAL-c2X/*AjPrdx4* and pMAL-c2X/*AjPrdx6* were transformed into the *Escherichia coli* (*E.coli*) DH5α competent cells and sequenced.

Table 1. Oligomers used in this study

Name	Purpose	Sequence (5'-3')
Aj-Prdx6-RTF	qPCR analysis of AjPrdx6	CTGCCCGCTGTGTGTTTGTGATT
Aj-Prdx6-RTR	qPCR analysis of AjPrdx6	GGCCACTCTTTGCTTTGCAGTCA
Aj-Prdx6-XpF	ORF amplification (<i>EcoRI</i>)	GAGAGAGaattcCCATGCCTGGAATATTGTTAGGAGACG
Aj-Prdx6-XpR	ORF amplification (<i>HindIII</i>)	GAGAGAAagcttTCATGGCTGGGGTGTGTAGC
Aj-EF1 α F2	qPCR for AjEf1-a	GAGGTCAAGTCTGTGGAAATGCAC
Aj-EF1 α R2	qPCR for AjEf1-a	TGATGACCTGAGCAGTGAAGGTAC
Aj-Prdx4-RTF	qPCR analysis of AjPrdx4	ACGACAGATCACCATGAACGACCTC
Aj-Prdx4-RTR	qPCR analysis of AjPrdx4	CAGTTTGCCAGAAGGGTCAGGGATTA
Aj-Prdx4-XpF	ORF amplification (<i>EcoRI</i>)	GAGAGAGaattcATGGACGGCCGACAGTACATG
Aj-Prdx4-XpR	ORF amplification (<i>HindIII</i>)	GAGAGAAagcttGGCATTCAAGGGTTCAATTCAGTTTGTGTC



2.9 Overexpression and purification of recombinant AjPrdx4 and AjPrdx6

After sequence confirmation of recombinant pMAL-c2X/AjPrdx4 and pMAL-c2X/AjPrdx6 were transformed into *E. coli* BL21 (DE3) competent cells and plated on agar. A single colony was selected and inoculated into 10 mL of Luria-Bertani (LB) broth containing ampicillin (100 μ g/mL) and incubated at 37°C shaking incubator for overnight. Then 5 mL from the overnight culture was inoculated into 500 mL of LB broth supplemented with ampicillin (100 μ g/mL) and glucose (0.2%) and grown at 37°C shaking incubator until the optical density reaches to 0.5 at 600 nm (OD₆₀₀). Thereafter expression of AjPrdx4 and AjPrdx6 fusion proteins were induced using 0.5 mM of isopropyl- β -thiogalactopyranoside (IPTG) and mixtures were incubated at 20°C for 8 h with shaking. Then, cells were harvested by centrifugation at 3500 \times g for 30 min at 4°C and subsequently resuspended in column buffer (20 mM TrisHCL, pH 7.4

and 200 mM NaCl) and stored at -20°C. The harvested cells were lysed by sonication and lysates were immediately subjected to the centrifugation at $3500 \times g$ for 30 min at 4°C. Using the pMAL™ protein fusion and purification system, the recombinant AjPrdx4 and AjPrdx6 proteins were purified according to the manufacture's instruction (New England BioLabs, Ipswich, MA, USA). Finally concentrations of purified recombinant proteins were determined by Bradford method. Moreover, resultant proteins were assayed using the 12% SDS-PAGE along with the standard molecular size marker and visualized with coomassie brilliant blue R250 following standard staining and de-staining procedures.

2.10 Cell culture

The vero (kidney epithelial cell from an African green monkey) cells from an established cell culture were used in this study. Briefly, the cells were cultured in growth medium of DMEM containing 10% heat inactivated FBS supplemented with penicillin (100 U/mL), streptomycin (100 µg/mL) and sodium pyruvate (110 mg/mL). The cells were incubated at 37°C in 5% CO₂ humidified incubator.

2.11 Protective effects of recombinant AjPrdx4/ AjPrdx6 on cultured cells under oxidative stress

In order to investigate cell protecting ability of rAjPrdx4/rAjPrdx6 fusion protein under oxidative stress, the cell viability assay was conducted. Cells were seeded at 2×10^5 /mL in 96 well plate and incubated for 24 h. Thereafter cells were pretreated with different concentrations of rAjPrdx4 or rAjPrdx6 fusion proteins, 1mM dithiothreitol (DTT) and incubated for 30 min. After the incubation 500 µmol H₂O₂ was added and incubated for 24h. Experimental treatments are as follows, (A) control cells, (B) 100 µg/mL of MBP with 1 mM of DTT + 500 µmol of H₂O₂, (C) 25 µg/mL of

rAjPrdx4-MBP or rAjPrdx6-MBP with 1 mM of DTT + 500 μmol of H_2O_2 , (D) 50 $\mu\text{g}/\text{mL}$ of rAjPrdx4-MBP or rAjPrdx6-MBP with 1 mM of DTT + 500 μmol of H_2O_2 , (E) 75 $\mu\text{g}/\text{mL}$ of rAjPrdx4-MBP or rAjPrdx6-MBP with 1 mM of DTT + 500 μmol of H_2O_2 and (F) 100 $\mu\text{g}/\text{mL}$ of rAjPrdx4-MBP or rAjPrdx6-MBP with 1 mM of DTT + 500 μmol of H_2O_2 . Then cell viability was determined by a standard 3-(4, 5-dimethylthiazol-2-yl) 2, 5-diphenyltetrazolium bromide (MTT) assay. During the MTT assay, yellow color tetrazolium bromide is converted into purple colored formazan derivative by mitochondrial succinate dehydrogenase presence in viable cells (Mosmann, 1983). After the 24 h incubation period the MTT solution (50 μL : 2 mg mL^{-1}) was added to the each well, to a total reaction volume of 200 μL and incubated for 3h. Thereafter supernatants were aspirated and 150 μL of dimethylsulfoxide (DMSO) was added to the each well to dissolve the formazan crystals. Then absorbance was measured by ELISA plate reader at wave length of 540 nm. Relative cell viability was calculated according to the amount of MTT converted to the insoluble formazan. The optical density of the formazan generated in the control cells were considered to 100% viability. The data are expressed as mean percentages of the viable cells versus the respective control.

3. RESULTS AND DISCUSSION

3.1. PART 1

Molecular Characterization of a 1-Cys Peroxiredoxin counterpart (Peroxiredoxin 6) from Japanese eel (*Anguilla japonica*); revealing its antioxidant properties and transcriptional modulation under pathogenic stress

3.1.1 Sequence characterization

The full length coding sequence of *AjPrdx6* was 669 bp in length (GeneBank accession no: KP246841), which encodes a polypeptide of 223 amino acids with a molecular weight of 24.9 kDa and theoretical isoelectric point of (PI) 5.32. The deduced *AjPrdx6* exhibited typical 1-cystine peroxiredoxin family domain architecture, including a redoxin domain profile (residues 35-163) and the N terminus active site (⁴⁴PVCTTE⁴⁹) with catalytic cysteine active site residue (peroxidatic cysteine) (C⁴⁶) (Fig. 5). Furthermore the catalytic triad residues that involved in peroxidase activity (H³⁸, C⁴⁶ and R¹³¹) and phospholipase A activity (H²⁵, S³¹ and D¹³⁹) (Fig. 5) were identified. The signal peptide was not identified in entire *AjPrdx6* amino acid sequence by signalP server, suggesting that the *AjPrdx6* might be localized in the cytosol. Although this observation was further confirmed by previous report from Wood et al 2003, revealed that the mammalian Prdx6 is localized only in cytosolic environments (Wood et al., 2003).

			AGTTGGTC	GAAAAAGTCGTAACC	23
<u>ATG</u> CCTGGAATATTG	TTAGGAGACGTTTTTC	CCAAACTTTGAAGCC	GAAACAACAATTGGC		83
M P G I L	L G D V F	P N F E A	E T T I G		20
AAGATCAAATTCCAC	GACTTTTTGGGAGAC	TCCTGGGGCGTCCCTG	TTCTCCCACCCCTCGT		143
K I K F H	D F L <i><u>G D</u></i>	<i><u>(S) W G V L</u></i>	F S H P R		40
GACTACACCCCTGTG	TGCACCACCGAGCTG	GGCCAAGCCGCCAAA	CTCAGCGACGAGTTC		203
D Y T <u>P V</u>	<u>C T T E</u> L	G Q A A K	L S D E F		60
AAGGAGCGCGATGTC	AAGATGATCGCGCTG	TCCGTCGACAGCGTG	GAGGATCACCGCGGC		263
K E R D V	K M I A L	S V D S V	E D H R G		80
TGGACTAAGGACATT	ATGGCCTACAATCAG	GAGGATCCC GGCTGT	CCTTTCCCTTTCCCC		323
W T K D I	M A Y N Q	E D P G C	P F P F P		100
ATCATTGCAGATGAC	AAGAGGGAGCTGGCG	GTGAAGCTGGGCATG	CTGGACCCAGATGAG		383
I I A D D	K R E L A	V K L G M	L D P D E		120
CGGGACAAAGACGGC	GTGCCACTCACTGCC	CGCTGTGTGTTTGTG	ATTGGCCCAGACAAG		443
R D K D G	V P L T A	R C V F V	I G P D K		140
AAGATGAAGCTGTCC	ATTCTGTACCCCGCC	ACGACAGGACGCAAC	TTTAACGAGCTGCTC		503
K M K L S	I L Y P A	T T G R N	F N E L L		160
CGGGTCATTGACTCC	CTGCAGCTGACTGCA	AAGCAAAGAGTGGCC	ACTCCTGTGCGATTGG		563
R V I D S	L Q L T A	K Q R V A	T P V D W		180
AAGCCTGGTGTGATCGA	GTCATGGTCCCTGCTT	AATGTTCCCTGAAGCT	GAGGCTTCAGCCCTT		623
K P G D R	V M V L P	N V P E A	E A S A L		200
TTCCCTGCTGGAGTT	TACACCAAGGAATA	CCCTCTGGGAAAAAG	TACTTGCGTACACA		683
F P A G V	Y T K E L	P S G K K	Y L R Y T		220
CCCCAGCC <u>TGA</u> AGG	AAAGCAAGTCTCCTG	TGATCATTGAAGAGT	GAAAAACAAGAACA		743
P Q P					223
AGACAGACCTGGGTC	AAATGCGCATTTGTT	TTGGGTTCAGGTAGT	TTTCTGAGCTCTGTT		803
GATCTTGCCTGGTGT	ATTTGAGCCTGTAAA	TTTACTAAAGCCCA	TATAGCCTGCAAGTA		863
TGACCAGAAGGTCAT	GACCACTTTTGTAGA	GTGTTTCATTGGTTC	TAATACACCAGACAG		923
GATCGGCAAAGCATG	GAAGGGTATTTGAAT	ACAAGACAAATGCGT	ATTTGACCCAGTTCT		983
GGTGGGAAATGATGA	TAAGCCAGCTGTAGA	TGTGGCGCACGCATG	AATGTGCAGTGTGTC		1043
GTATTTGCAGGTTTG	CAGGTTTGCAGCTGT	GGCTGCGTGCCGCAG	CCCAGTTGAGCATGA		1103
ATGCAAACCGCCGCT	GTTGCTCAGCTGGCC	GTGCTACACAGAGAC	GGAAGTCGAGCAAAA		1163
CACCAGTTTCCTGTA	TCCCTCCCCACCCA	CACTGAGATGCGAGA	GAACGCCGAGATGGG		1223
TGGGTTTGGGGCGAA	GCAGGTGGCTGGTCC	AGGAACCTGTATGTT	GTAGGCCCTGGACTA		1283
TGACATGATTAATGA	ACTGAACCATATTTA	AGTGGGACTCTAATG	AAGTGTCCCTTGTG		1343
AGCTTGAACTACACT	CTACTGTGTTCCATG	CGATGTGTACAGATG	AGTATGTACGTGCAC		1403
TTGAATGCATTGTGA	GACTGTAGCGCCATG	TGTAATTAGTAAATA	CATGTACATTATTGG		1483
AGAACACTTGACTGA	GCACCTCACCA				1509

Fig.5. The nucleotide and deduced amino acid sequences of Japanese eel, *Anguilla japonica* Prdx6. The start (ATG) and stop (TGA) codons are bold and underlined. The redoxin domain profile is shaded with gray color. The peroxidase catalytic active site (⁴⁴PVCTTE⁴⁹) is bold and underlined. The peroxidatic cysteine residue C⁴⁶ is boxed. Conserved active site for phospholipase A2 activity (²⁹GDSWG³³) is italic and underlined. The Phospholipase A2 catalytic residue is depicted by circle. Important amino acids involved in peroxidatic catalytic triad are marked by hexagon, whereas the amino acid residues in phospholipase A2 catalytic triad are indicated by pentagons.

The EMBOSS needle pairwise sequence alignment showed that the deduced AjPrdx6 amino acid sequence has greatest amino acid identity (82.5%) to that of *Salmo salar*, followed by *Oplegnathus fasciatus* (81.2%), *Scophthalmus maximus* (81.2%),

Oncorhynchus mykiss (80.3%), *Ictalurus punctatus* (78.9%), *Danio rerio* (77.6%), *Xenopus laevis* (79.5%), *Gallus gallus* (75.9%), *Homo sapiens* (75.0%), *Bos taurus* (74.6%) (Table. 2). According to the report from Manevich et al 2005, the Prdx6 has more than 95% amino acid and nucleotide similarity among the mammals (Human, pig, rat, mouse and cow) (Manevich and Fisher, 2005). Likewise we observed more than 90% amino acid similarity of Prdx6 among the fish species considered herein.

Table 2. Pairwise identity and similarity percentages of AjPrdx6 with selected orthologs at amino acid level

Species	Accession No.	Identity (%)	Similarity (%)	Amino acids
<i>Salmo salar</i>	ACI67008	82.5	93.3	223
<i>Oplegnathus fasciatus</i>	ADJ21808	81.2	92.4	221
<i>Scophthalmus maximus</i>	ADJ57694	81.2	91.9	223
<i>Oncorhynchus mykiss</i>	NP_001158604	80.3	91.0	222
<i>Ictalurus punctatus</i>	NP_001187160	78.9	90.1	223
<i>Danio rerio</i>	NP_957099	77.6	91.9	222
<i>Xenopus laevis</i>	NP_001082669	79.5	89.3	224
<i>Gallus gallus</i>	NP_001034418	75.9	87.1	224
<i>Homo sapiens</i>	NP_004896	75.0	87.1	224
<i>Bos taurus</i>	NP_777068	74.6	87.1	224

The clustalW2 multiple sequence alignment was performed to compare the homology between Prdx6 counterparts from fish, mammals, amphibians and avian (Fig. 6). The redoxin domain profile of AjPrdx6 was highly conserved with all vertebrate Prdx6 counterparts considered herein. Interestingly, the N-terminus catalytic active site (⁴⁴PVCTTE⁴⁹) including peroxidase catalytic center (C⁴⁶) of AjPrdx6 was completely conserved with all the vertebrate Prdx6 counterparts tested. Moreover, the catalytical triads that involved in peroxidase activity (H³⁸, C⁴⁶ and R¹³¹) and phospholipase A activity (H²⁵, S³¹ and D¹³⁹) of AjPrdx6 were 100% conserved among selected Prdx6 counterparts from fish, mammalians, avian and amphibians (Fig. 6). Altogether these observations infer that the AjPrdx6 is an indeed homolog of Prdx6 subclass and

3.1.2. Phylogenetic analysis

The phylogenetic analysis was conducted to determine the molecular evolutionary relationship of AjPrdx6 with known Prdx subclasses from fish, birds, mammals and amphibians using the neighbor joining method (Fig. 7). As expected three major clades corresponding to typical 2-Cys Prdxs (Prdx1-Prdx4), 1-Cys Prdx (Prdx6) and atypical 2-Cys Prdxs (Prdx5) were observed (Fig. 7). Interestingly, the typical 2-Cys Prdx clade was joined to the 1-Cys Prdx clade, while the atypical 2-Cys Prdx class was clustered as a separate branch (Fig. 7). This discrete clustering pattern suggested that the atypical 2-Cys Prdx subclass is distantly related to the typical 2-Cys Prdx and typical 1-Cys Prdxs. In addition, this observation is a substantial evidence to prove that the closer evolutionary relationship in genetic structure of members of typical 2-Cys Prdx subclass (Prdx1, Prdx2, Prdx3 and Prdx4) (Ren et al., 2013). As depicted in Fig. 7, the AjPrdx6 was positioned in the piscine sub group of 1-Cys Prdx clade exhibiting a highest evolutionary proximity to *S.salar* Prdx6. As well as Prdx6 counterparts from mammals, avians and amphibians were separately clustered in their corresponding sub-clades in the 1-Cys Prdx main clade. Therefore, our phylogenetic study revealed that the AjPrdx6 has been evolved from common vertebrate origin.

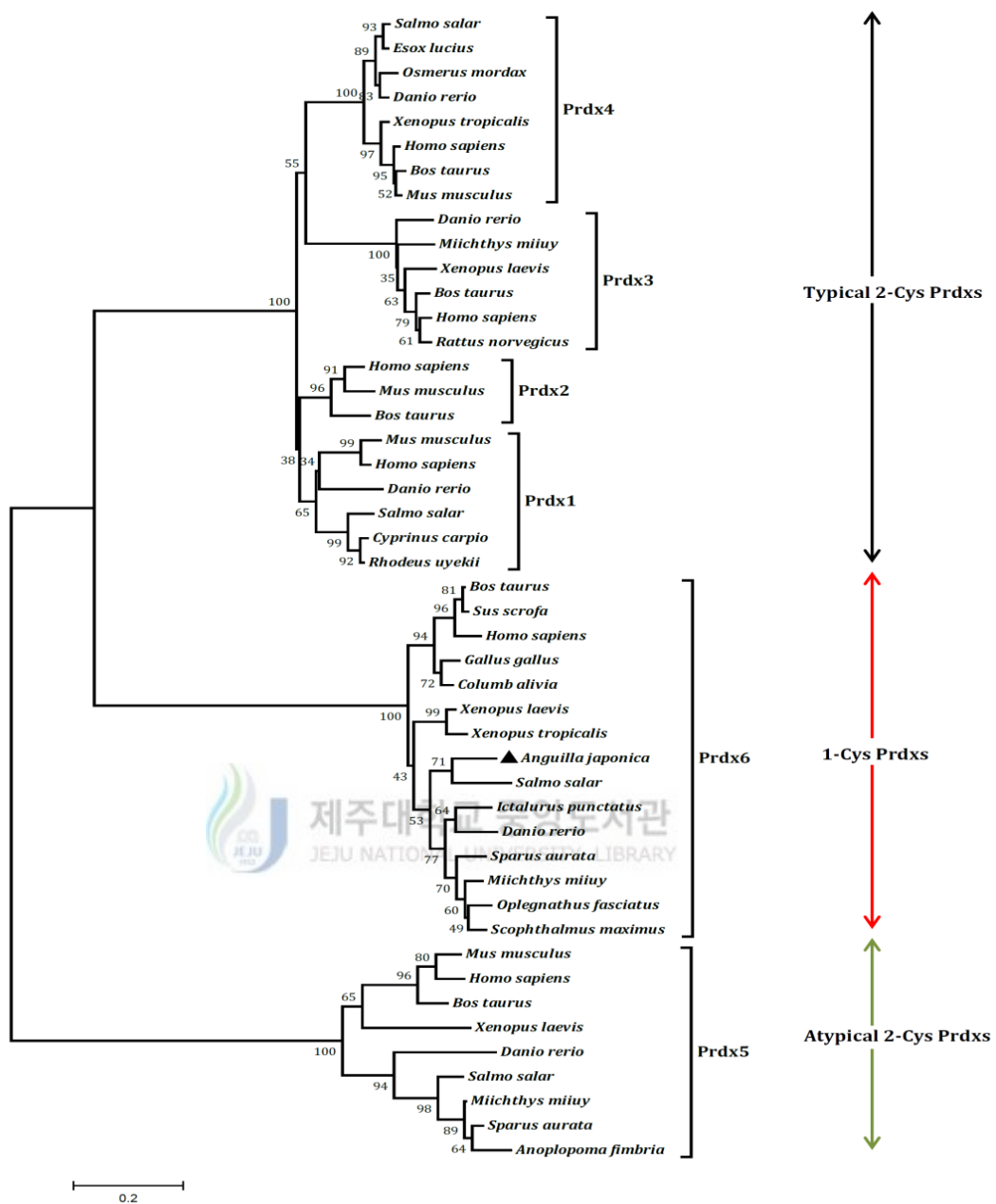


Fig. 7. Phylogenetic tree of known Prdxs from different species including the AjPrdx6. The tree was constructed using the multiple alignment of overall sequences by neighbor-joining method. Bootstrap values are shown next to the branches based on 1000 replications.

3.1.3. Predicted 3D homology modal of AjPrdx6

The 3D structural modal of AjPrdx6 protein was generated by ITASSER online server (Zhang, 2008) using top ten compatible templates from the Research

Collaboratory for Structural Bioinformatics (RCSB) protein data bank. All the obtained templates exhibited higher identity (67%- 75%) to the query sequence, as well as normalized Z- score of the threading alignment was more than one. Those observations confidently prove that the reliability of predicted modal of AjPrdx6. Moreover the generated modal of AjPrdx6 showed 0.94 ± 0.05 of estimated TM score and 1.62 of confidence score (C- Score), suggesting that it's closer similarity to the native structure of known Prdx6 (Zhang, 2008). The retrieved modal of AjPrdx6 was visualized using the PyMOL molecular graphic software. The tertiary structure of AjPrdx6 was composed of nine core stranded β -sheets flanked by seven α -helices (Fig. 8A). The C-terminus, N-terminus and redoxin domain profile were identified in the generated modal of AjPrdx6 (Fig. 8A). Furthermore, the active site cysteine residue (C^{46}), catalytical triads that involved in peroxidase activity (H^{38} , C^{46} and R^{131}) and phospholipase A activity (H^{25} , S^{31} and D^{139}) were identified (Fig. 8B). Crystal structure analysis of human Prdx6 identified C^{47} , H^{39} and R^{132} as catalytic triad for peroxidase activity; the peroxidatic C^{47} form a hydrogen bond with H^{39} in peroxidase catalytic triad and R^{132} is involve in electrostatically activation of C^{47} (Hamza, 2002; Hofmann et al., 2002). According to the generated modal of AjPrdx6, corresponding amino acid residues for peroxidase catalytical triad of AjPrdx6 (H^{38} , C^{46} and R^{131}) were positioned in same plane and adjacent to each other (Fig. 8B). In human the Prdx6 also contain a catalytical triad for phospholipase A2 activity (H^{25} , S^{31} and D^{139}) (Manevich and Fisher, 2005). Crystal structure analysis of human Prdx6 demonstrated that the catalytic C^{47} was positioned at 25Å away from the phospholipase A2 catalytic center (S^{32}), thereby prohibits the interaction of two active centers for different activities (Choi et al., 1998). Likewise we observed the two catalytic active centers that responsible for peroxidase activity (C^{46}) and phospholipase A2 activity (S^{31}) at two significantly different positions

in the generated modal of AjPrdx6 (Fig. 8B). Collectively these finding demonstrated that the 3D arrangement of AjPrdx6 is compatible with its function.

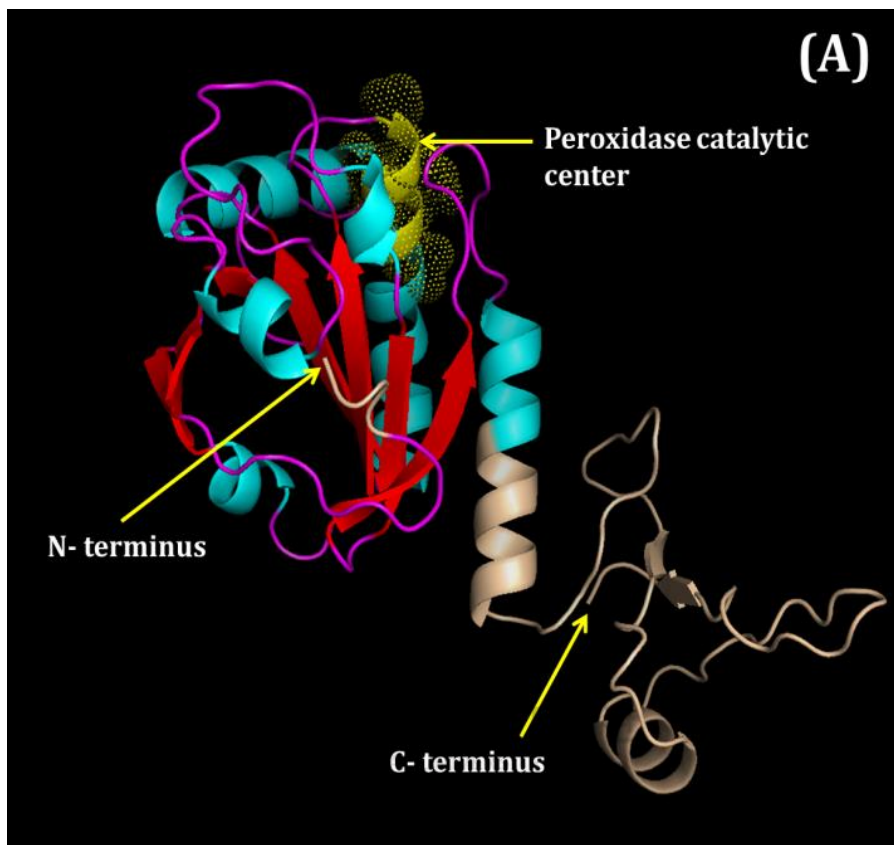


Fig. 8A. Computer simulation model generated for the AjPrdx6. Tertiary structure elements belonging to the redoxin domain profile: (sky blue) α -helixes, (Red) β -sheets. The peroxidase catalytic center is represented with yellow dots.

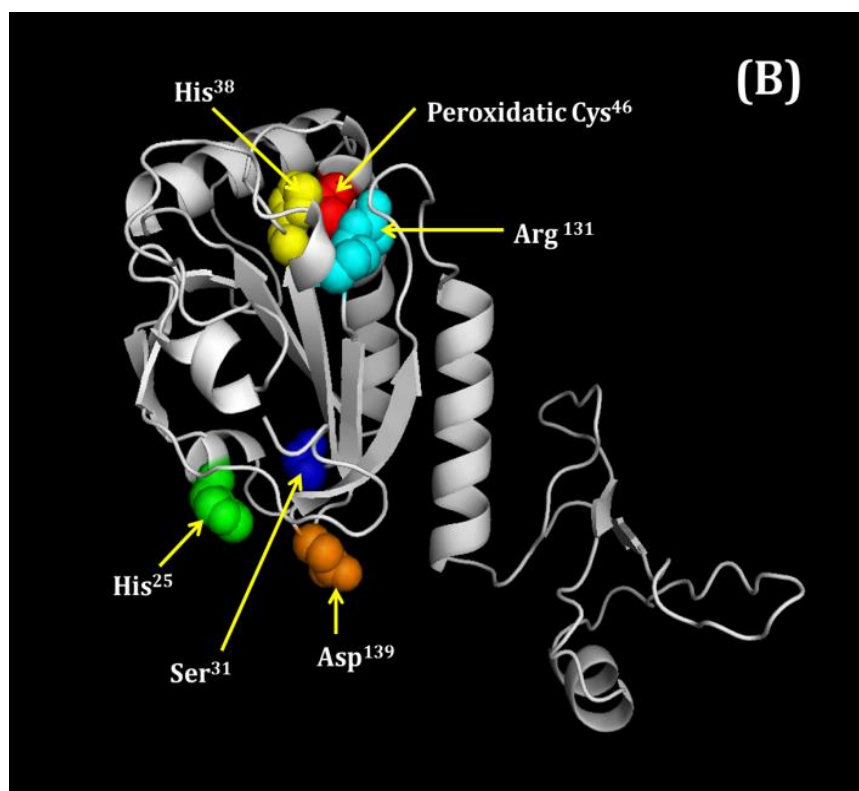


Fig. 8B. 3D structure of AjPrdx6 with important conserved amino acid residues. The Peroxidatic Cys⁴⁶ is marked with red color sphere, whereas and rest of the amino acid residues in catalitical triad for peroxidase activity are marked with yellow (His³⁸) and sky blue (Arg¹³¹) spheres. The corresponding conserved amino acid residues for phospholipase A2 catalytic triad are denoted by green (His²⁵), blue (Ser³¹) and orange (Asp¹³⁹) spheres

3.1.4. Tissue distribution analysis of *AjPrdx6*

Tissue specific distribution of *AjPrdx6* mRNA transcripts in healthy Japanese eels were determined by qPCR analysis using *Anguilla japonica* Elongation Factor 1-Alpha (*AjEF1-a*) as an internal control. Expression fold of *AjPrdx6* in each tissue was calculated relative to spleen. The *AjPrdx6* was ubiquitously expressed in all the immune and non-immune tissues examined, including Liver, spleen, brain, muscle, heart, skin, kidney, head kidney, gill, gonad and intestine (Fig. 9). As shown in Fig. 9, *AjPrdx6* was highly expressed in muscle followed by heart, gill and brain, while lowest expression fold was detected in spleen (Fig. 9). Wen- jiang Zheng and group revealed that *Prdx6* was highly expressed in blood, heart and muscle among the tested tissues of turbot

(*Scophthalmus maximus*); however lowest level was detected in spleen (Zheng et al., 2010). Expression of rock bream (*Oplegnathus fasciatus*) *Prdx6* was predominantly detected in liver followed by intestine, while lowest in spleen, skin and gill (De Zoysa et al., 2012). Therefore, we can speculate that the tissue specific expression of *Prdx6* was depending on the fish species. On the other hand developmental stage and genetic background of the fish might be attributed to the different tissue specific distribution pattern of the *Prdx6* in each fish species.

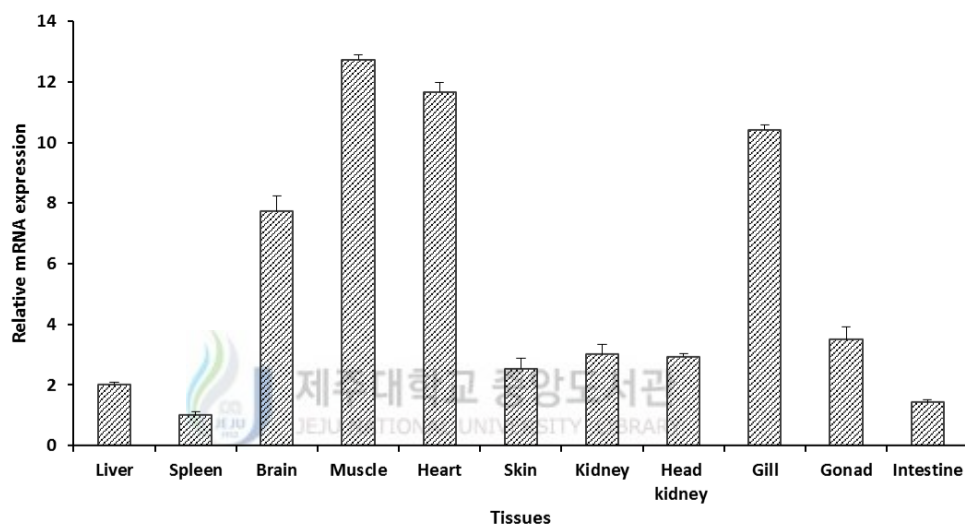


Fig. 9. Tissue specific expression analysis of *AjPrdx6* mRNA in healthy *Anguilla japonica* by qPCR. The mRNA expression level of each tissue is expressed relative to the mRNA expression in skin tissue. Each bar represents the standard error (SE) of triplicates (n = 5).

3.1.5. Expression profile of *AjPrdx6* upon *E. tarda*, LPS and Poly I:C challenge

In order to determine the innate immune responses of *AjPrdx6* upon different stimuli, healthy Japanese eels were challenged with gram negative fish pathogen *E. tarda*, LPS and Poly I:C. Thereafter the relative mRNA expression profile of *AjPrdx6* in liver and spleen was determined by quantitative real-time PCR (qPCR) using *Anguilla japonica* Elongation Factor 1-Alpha (*AjEF1-a*) as an internal control gene. The liver and spleen are believed to play pivotal role in early innate immune responses against pathogenic infections in vertebrates, and several researchers have selected

those tissues as target tissues for determine the temporal mRNA expression profile of innate immune related genes. Therefore we selected liver and spleen as candidate tissues for investigate the expressional profile of *AjPrdx6* mRNA transcripts upon *E.tarda*, LPS and poly I:C challenge. Only one peak of both *AjPrdx6* and *AjEF1-a* was detected at corresponding melting temperature in the dissociation curve analysis, suggesting that the target was specifically amplified. As shown in Fig. 10A. the mRNA transcripts of *AjPrdx6* were gradually upregulated until 48 h post injection of *E. tarda* with significant ($P<0.05$) inductions at 12 h, 24 h, 48 h and 72 h post injection (p.i). After the LPS stimulation gradual up-regulation of *AjPrdx6* transcripts were detected at early to middle phase of p.i, nevertheless up-regulation was fluctuated at latter phase of p.i. Moreover, significant up-regulations were detected at 6 h, 12 h and 24 h after p.i of LPS (Fig. 10B). As well as the basal mRNA transcript levels of *AjPrdx6* were significantly elevated at 3 h, 6 h and 24 h p.i. upon the Poly I:C injection (Fig. 10C).



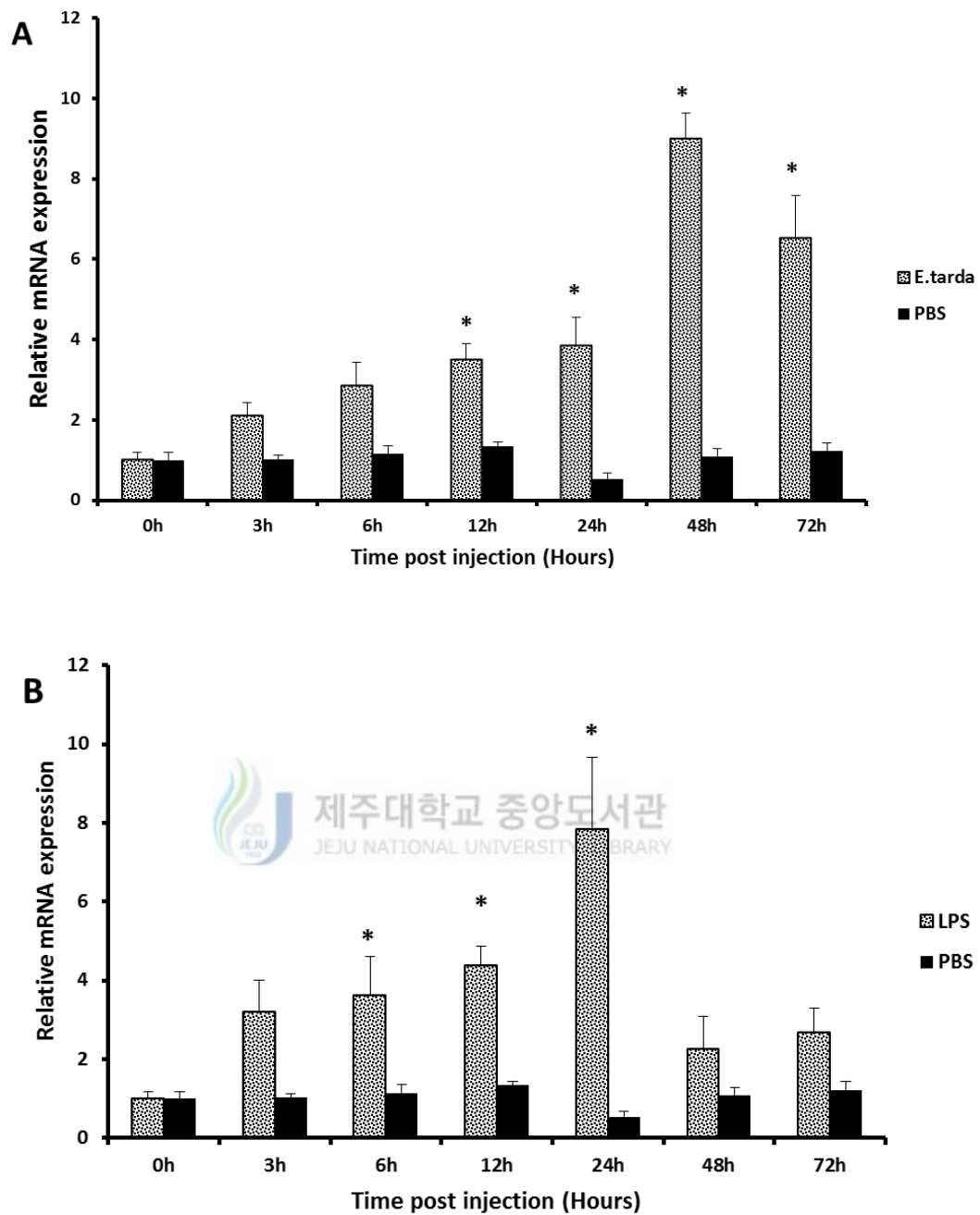


Fig. 10A,B. Relative mRNA expression pattern of *AjPrdx6* in liver after the stimulation with *Edwardsiella tarda* (A) and LPS (B) The expression analysis of *AjPrdx6* was determined by SYBR green quantitative real time PCR. Livak $2^{-\Delta\Delta CT}$ method was used to calculate relative expression levels using *Anguilla japonica EF-1a* as internal control gene. Each bar represents the standard error (SE) of five individual samples (n=5). Asterisk (*) represents the significant difference in expression against the un-injected control ($p < 0.05$).

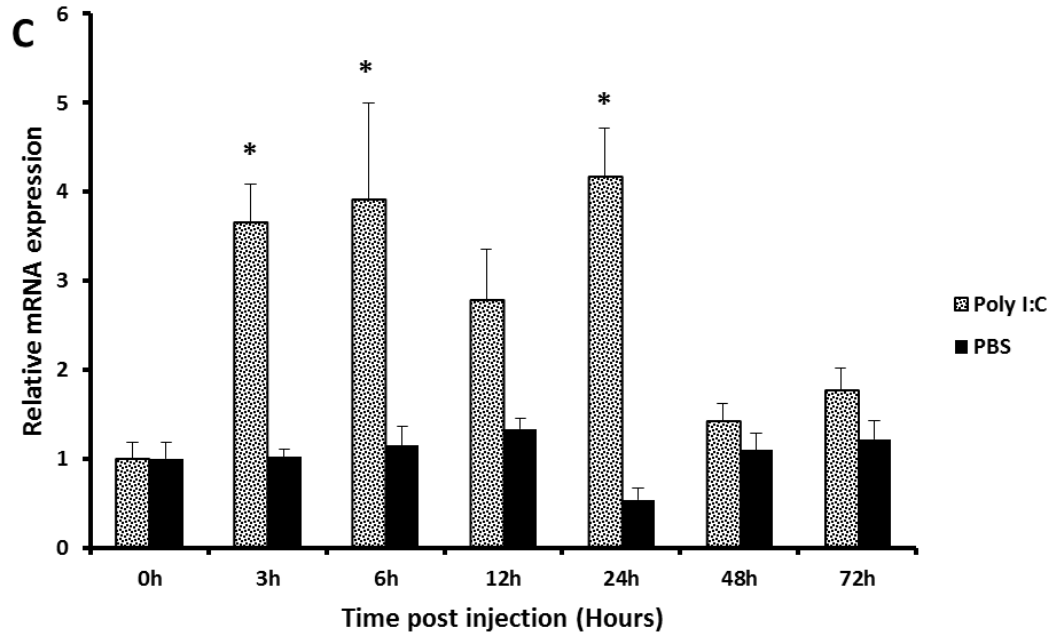


Fig. 10 C. Relative mRNA expression pattern of *AjPrdx6* in liver after the stimulation with Poly I:C. The expression analysis of *AjPrdx6* was determined by SYBR green quantitative real time PCR. Livak $2^{-\Delta\Delta CT}$ method was used to calculate relative expression levels using *Anguilla japonica EF-1a* as internal control gene. Each bar represents the standard error (SE) of five individual samples (n=5). Asterisk (*) represents the significant difference in expression against the un-injected control (P < 0.05).

As depicted in Fig. 11A, after the injection of *E. tarda* the *AjPRdx6* mRNA transcripts were upregulated throughout the experiment, while significant upregulations were observed at 48 h and 72 h p.i in spleen tissues. However the *AjPrdx6* mRNA transcripts were gradually upregulated until 12 h p.i with the significant inductions at 6 h and 12 h after the LPS injection in spleen tissues (Fig. 11B). Nevertheless the expression pattern was fluctuated after reaching to the maximum induction fold. Moreover *AjPrdx6* transcripts were down-regulated at 48 h and 72 h p.i after the LPS injection in spleen tissues (Fig. 11B). In spleen, poly I:C injection engendered significant upregulation of *AjPrdx6* mRNA transcripts at 3 h and 12 h p.i, while the expression fold was down regulated at 48 h p.i (Fig. 11C).

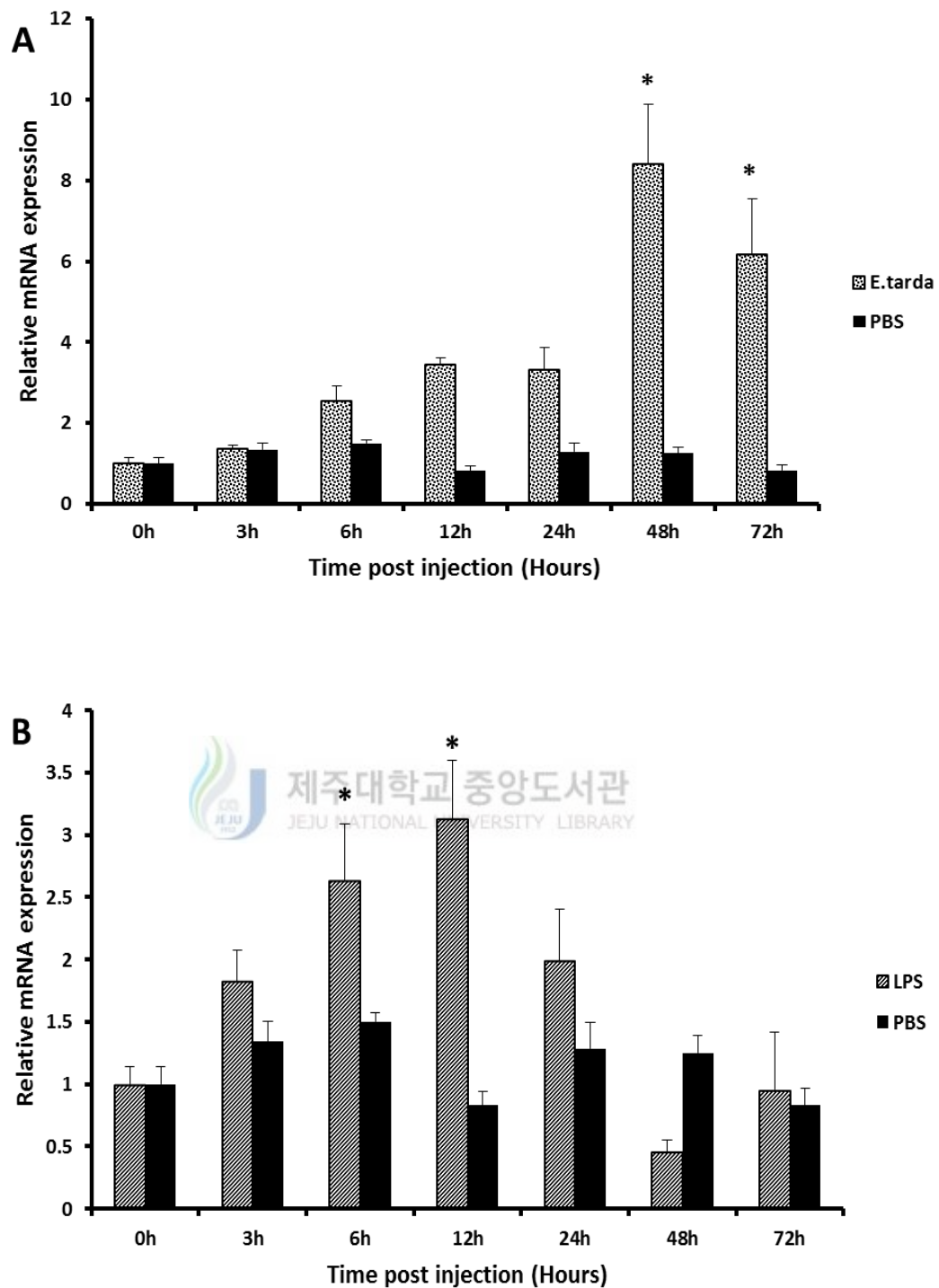


Fig. 11A.B. Relative mRNA expression pattern of *AjPrdx6* in spleen after the stimulation with *Edwardsiella tarda* (A) and LPS (B). The expression analysis of *AjPrdx6* was determined by SYBR green quantitative real time PCR. Livak $2^{-\Delta\Delta CT}$ method was used to calculate relative expression levels using *Anguilla japonica EF-1a* as internal control gene. Each bar represents the standard error (SE) of five individual samples (n=5). Asterisk (*) represents the significant difference in expression against the un-injected control ($p < 0.05$).

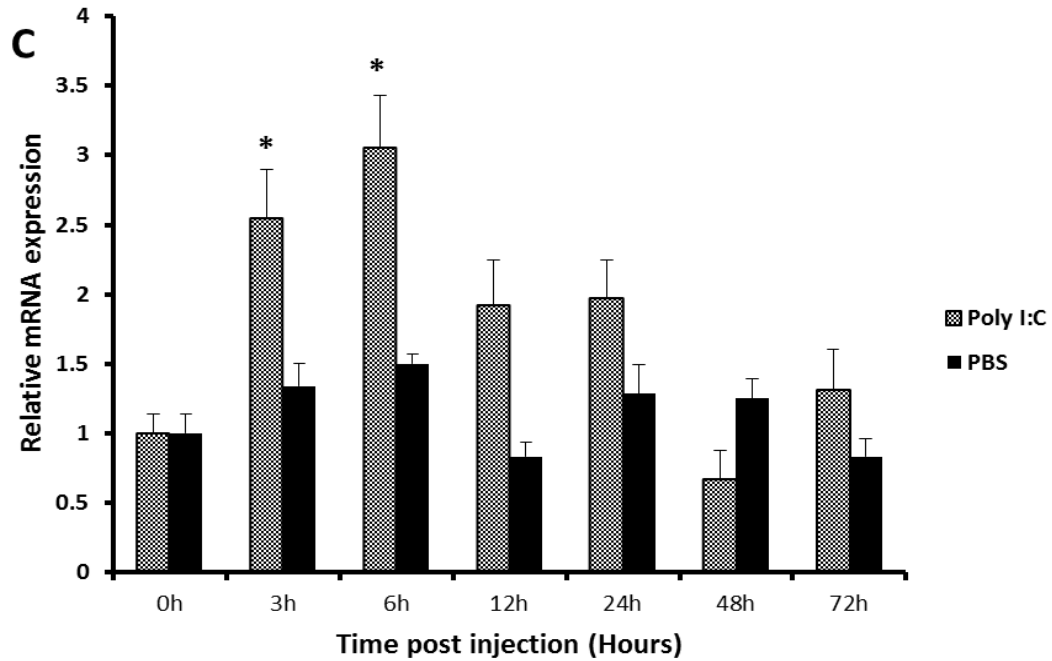


Fig. 11C. Relative mRNA expression pattern of *AjPrdx6* in spleen after the stimulation with Poly I:C. The expression analysis of *AjPrdx6* was determined by SYBR green quantitative real time PCR. Livak $2^{-\Delta\Delta CT}$ method was used to calculate relative expression levels using *Anguilla japonica EF-1a* as internal control gene. Each bar represents the standard error (SE) of five individual samples (n=5). Asterisk (*) represents the significant difference in expression against the un-injected control ($p < 0.05$).

Several previous studies have demonstrated that up-regulation of *Prdx6* transcription under various pathological conditions in many organisms including teleost. However, reports on *Prdx* in *anguillidae* species are relatively scarce. Wen-jiang Zheng and group demonstrated that, upregulation of *Prdx6* mRNA transcripts upon *Listonella anguillarum* and Poly I:C injections in the spleen and liver tissues of *Scophthalmus maximus* (Zheng et al., 2010). Furthermore, it has been shown up-regulation of *Prdx6* mRNA transcripts in liver tissue of *Oplegnathus fasciatus* after the Poly I:C injection (De Zoysa et al., 2012). Interestingly mRNA expression pattern (except the fold difference) of *O. fasciatus* in liver after the Poly I:C injection (De Zoysa et al., 2012) was quite similar to that of our results shown in Fig. 11C. Nevertheless, down regulations of *Prdx6* in gill tissues of disk abalone against viral infection (Nikapitiya et al., 2009) and haemocytes in *Eriocheir sinensis* (chinese mitten crab) upon *L.*

anguillarum injection have also been reported (Mu et al., 2009). Moreover numerous studies have implicated that expression of *Prdx6* could be regulated in several organisms due to several stress conditions, like thermal exposure (Park et al., 2008) and environmental pollutants (David et al., 2007).

In this study, almost similar expression profiles of *AjPrdx6* mRNA were observed in liver and spleen tissues upon *E. tarda* injection (Fig. 10A & Fig. 11A). *E. tarda* is a potent gram negative fish pathogen (Ling et al., 2000) which could be detected by pathogen recognition receptors through pathogen associated molecular patterns (PAMPs). The LPS, is a pivotal PAMP in gram negative bacteria, which can induce the potent immune response in host after being recognized by toll like receptor 4 (TLR4). Thereafter, phagocytes and macrophages are activated and induce the production of ROS to counterattack the pathogenic invasion (Yang et al., 2007; Kaihami et al., 2014). In order to scavenge excess ROS or maintain the cellular oxidative stress under the pathological condition, transcription of peroxidases should be induced. Previous studies revealed that up-regulation of *Prdx6* in liver cells of mouse under H₂O₂ stress (Gallagher and Phelan, 2007). Moreover Dong Yang and group investigated *Prdx6* knockout mice were susceptible for acute oxidative stress after LPS challenge, thereby induce the lung injury compared to wild type mice (Yang et al., 2011). Regarding to the above mentioned facts, we suggested up-regulation of *AjPrdx6* mRNA transcripts might be due to the detection of PAMPs in *E. tarda* by PRRs in phagocytes or macrophages in liver and spleen. As depicted in Fig. 10A & Fig 11A, the *AjPrdx6* mRNA transcripts were gradually up-regulated and reached maximum induction fold at 48 h p.i of *E. tarda* in both liver and spleen. The lower induction fold of *AjPrdx6* mRNA transcripts at 3 h-24 h p.i could be attributed the fact of immune evasion mechanism elicited by pathogen to overcome host immune response.

According to the phenomena of pathogen evasion, bacteria like *E. tarda* can reduce intracellular ROS production in host (Borjesson et al., 2005). Therefore expression of antioxidant enzymes including *Prdx6* may be suppressed at early phase of post injection period of *E. tarda*. However, with the time host cells aroused sophisticated immune responses to counterattack the bacterial invasion; thereby *AjPrdx6* mRNA transcripts were highly up-regulated at latter phase of experiment upon *E. tarda* injection in liver and spleen. Interestingly after LPS injection, the *AjPrdx6* mRNA transcripts were also up-regulated in the liver (3 h-72 h p.i) and spleen (3 h-24 h p.i) (Fig. 10B & 11B), whereby proved our previous suggestions. Nevertheless, the fold difference of *AjPrdx6* induction at the early phase of *E. tarda* injection was comparatively lower than that of the LPS injection in liver. This observation was also correlated with previously discussed immune evasion mechanism of *E. tarda*.

The expression profile of *AjPrdx6* in liver upon Poly I:C injection was quite similar to that of spleen. Poly I:C is a double stranded RNA mimic which is sensed by TLR3 and ultimately induce production of type 1 interferones (IFNs) and proinflammatory cytokines (Alexopoulou et al., 2001). Previous reports documented that RNA virus could enhance production of the ROS after infection to host, thereby the antioxidant system is activated to protect the host from oxidative damage (Reshi et al., 2014). This hypothesis is in accordance with the fact that up-regulation of *AjPrdx6* mRNA transcripts upon Poly I:C injection in spleen and liver.

3.1.6. Over expression and purification of recombinant AjPrdx6

In order to characterize the antioxidant properties of AjPrdx6, the coding sequence was cloned into the pMAL-c2X expression vector and expressed as a fusion protein with MBP (Fig. 12). SDS-PAGE resolved a single purified protein band, confirming successful purification of the fusion protein and indicating a molecular mass of ~67 kDa. The size of the band was consistent with the predicted molecular mass of AjPrdx6 (24.9 kDa), since the molecular mass of MBP is ~42.5 kDa.

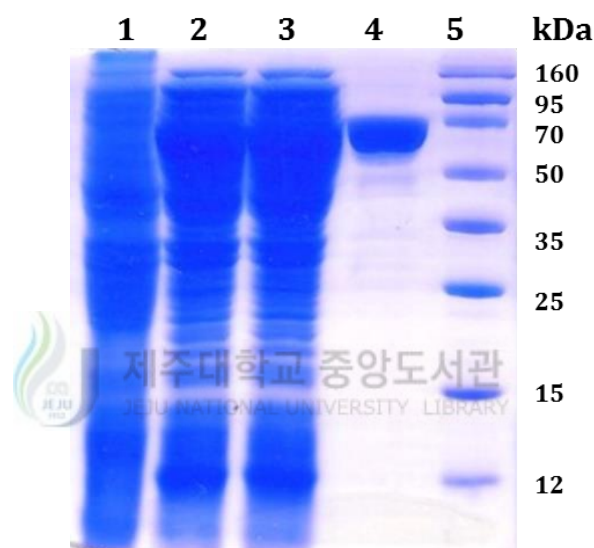


Fig. 12. SDS-PAGE analysis of the rAjPrdx6 fusion protein in *E. coli* BL21. Lanes 1, total protein of un-induced *E. coli* (BL21); lane 2, total cellular extract from *E. coli* BL21 carrying the rAjPrdx6-MBP expression vector after to IPTG; lane 3, soluble fraction; lane 4, purified recombinant fusion protein (rAjPrdx6-MBP) after IPTG induction; Lane 5, molecular weight marker.

3.1.7. Protective effects of recombinant AjPrdx6 (rAjPrdx6) on cultured cells under oxidative stress

The cytotoxic effect of H₂O₂ (100 mM) on vero (African green monkey kidney epithelial cells) cells in the presence of purified rAjPrdx6-MBP fusion protein with different concentrations were determined by MTT assay. The Prdxs are considered as

a thiol dependant enzymes, which required action of the electron donor like thioredoxin, glutaredoxin, cyclophilin or glutathione for complete their catalytic cycle (Sutton et al., 2010). Therefore DDT was used as an electron donor for this experiment. According to the results up to 50% cells survival was observed in rAjPrdx6 fusion protein treated cell samples under the H₂O₂ induced oxidative stress (Fig.13A). The MBP treated cells did not show significant cell viability compared to the rAjPrdx6 un-treated cells (Fig.13A. column 2). Moreover, microscopic images showed that, rAjPrdx6 untreated cells were severely damaged after H₂O₂ treatment (Fig.13A), while rAjPrdx6 pretreated cells were survived under oxidative stress (Fig.13C). Furthermore cell viability was not increased with the concentration of rAjPrdx6 fusion protein. Cell protecting ability of the Prdx6 under oxidative stress has been proved by previous experiments, for example, C. Nikapitiya et al 2009 and W.-j. Zheng et al 2010 described that H₂O₂ scavenging ability of recombinant Prdx6 from disk abalone and turbot respectively (Nikapitiya et al., 2009; Zheng et al., 2010). Altogether these observations along with the previous evidences suggested that the potency of rAjPrdx6 on cell protection under H₂O₂ mediated oxidative stress by reducing harmful H₂O₂ into nontoxic H₂O. Also we can speculate that the AjPrdx6 is expressed as an active form and exert their potent antioxidant nature under oxidative stress in Japanese eel.

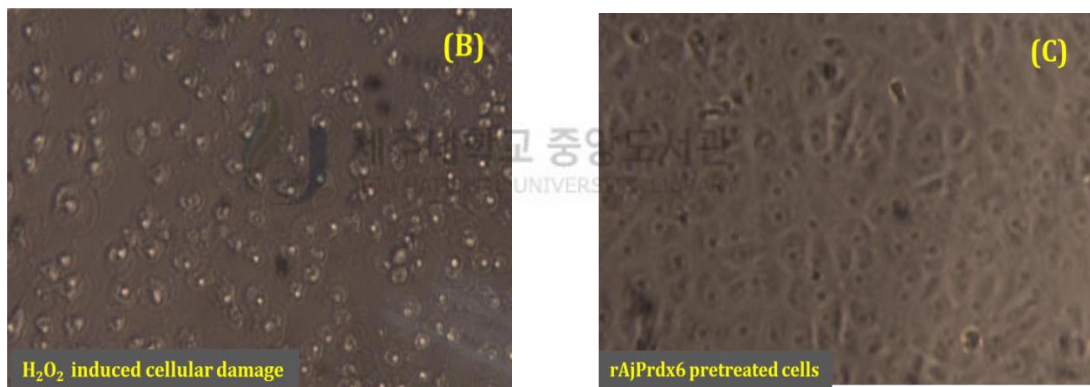
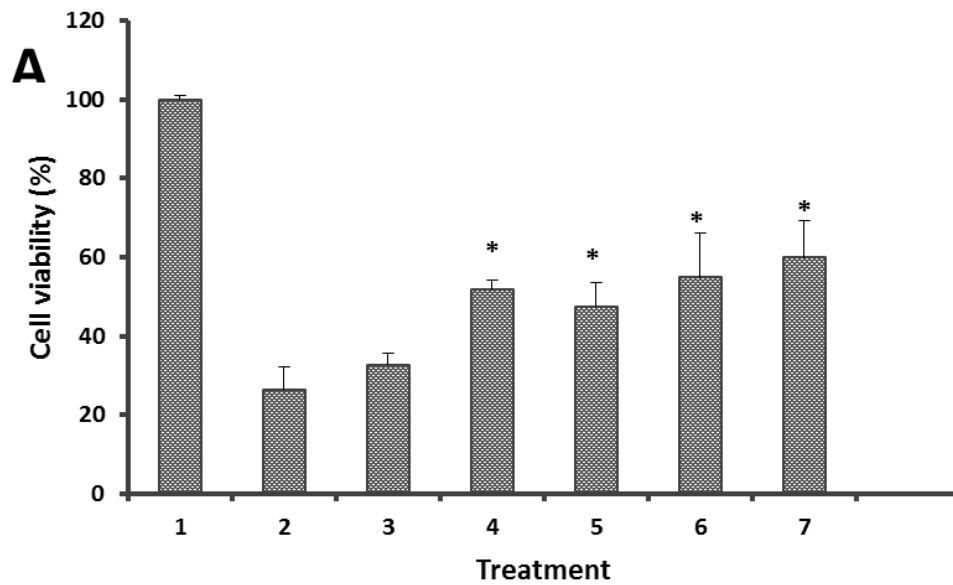


Fig. 13. (A) Effects of recombinant AjPrdx6 on cell growth and viability in 500 μM H_2O_2 exposed to vero cells. Cells were seeded at $2 \times 10^5/\text{mL}$ and pretreated with the different concentration combinations of rAjPrdx6 for 30 min followed by treatment with 500 μM H_2O_2 for 24 h. Cell viability was determined by MTT assay. Treatments: (1) control cells; (2) cells treated with H_2O_2 (500 μM); (3) cells pretreated with MBP (100 $\mu\text{g}/\text{mL}$) and DTT (1 mM) followed by H_2O_2 (500 μM); (4) cells pretreated with rAjPrdx6 (25 $\mu\text{g}/\text{mL}$) and DTT (1 mM) followed by H_2O_2 (500 μM); (5) cells pretreated with rAjPrdx6 (50 $\mu\text{g}/\text{mL}$) and DTT (1 mM) followed by H_2O_2 (500 μM); (6) cells pretreated with rAjPrdx6 (75 $\mu\text{g}/\text{mL}$) and DTT (1 mM) followed by H_2O_2 (500 μM); (7) cells pretreated with rAjPrdx6 (120 $\mu\text{g}/\text{mL}$) and DTT (1 mM) followed by H_2O_2 (500 μM). Each bar represents the standard error (SE) of three individual samples ($n=3$). Asterisk (*) represents the significant difference in cell viability against the control ($p < 0.05$). (B) Microscopic image of vero cells after the H_2O_2 (500 μM) treatment corresponding to the treatment no 2 in Fig A; (C) Microscopic image of rAjPrdx6-MBP (50 $\mu\text{g}/\text{mL}$) pretreated vero cells with DTT (1 mM) followed by H_2O_2 (500 μM) corresponding to treatment no 6 in Fig A.

3.2. PART-2

Typical 2-Cys Peroxiredoxin isoform (Peroxiredoxin 4) from Japanese eel (*Anguilla japonica*); Molecular characterization, mRNA expression and its protective roles against oxidative stress

3.2.1. Sequence characterization

Anguilla japonica peroxiredoxin 4 (*AjPrdx4*) was identified from previously constructed *Anguilla japonica* cDNA library. The full Open Reading Frame (ORF) of *AjPrdx4* was 786 bp (GeneBank accession no: KP246842) in length, which encodes a polypeptide of 262 amino acids with a molecular weight of 29.3 kDa and theoretical isoelectric point of (PI) 6.45. SAMRT server analysis revealed that *AjPrdx4* bears a characteristic redoxin domain profile (residues 71-222) (Fig.14). Moreover N-Terminus catalytic active center (¹¹¹FTFVCPTEI¹²⁰) and C-terminus active center (²³³GEVCPAGW²⁴⁰) were identified in *AjPrdx4* amino acid sequence (Fig.14). Furthermore conserved peroxidatic cysteine residues C¹¹⁵ and conserved resolving cysteine residue C²³⁶ were identified at N-terminus and C-terminus catalytic active centers respectively (Fig.14). The signal peptide was identified in entire *AjPrdx4* amino acid sequence by signalP server, revealing that the *AjPrdx4* was a secretory protein.

conserved with Prdx4s from fish, mammals and amphibians (Fig. 15). Collectively those observations suggested that AjPrdx4 is an indeed homolog of Prdx4 family.

Table 3. Pairwise identity and similarity percentages of AjPrdx4 with selected orthologs at amino acid level.

Species	Accession No.	Identity (%)	Similarity (%)	Amino acids
<i>Salmo salar</i>	ACI69656	88.9	93.5	262
<i>Esox lucius</i>	ACO14427	88.2	91.6	262
<i>Osmerus mordax</i>	ACO09915	87.8	91.2	261
<i>Danio rerio</i>	NP_001082894	84.1	88.1	260
<i>Larimichthys crocea</i>	ADJ67991	83.6	87.4	260
<i>Xenopus (Silurana) tropicalis</i>	NM_001006811	75.0	80.7	271
<i>Mus musculus</i>	NM_016764	74.5	83.6	274
<i>Homo sapiens</i>	EAW98996	73.5	82.1	271
<i>Bos taurus</i>	NM_174433	72.2	81.2	274



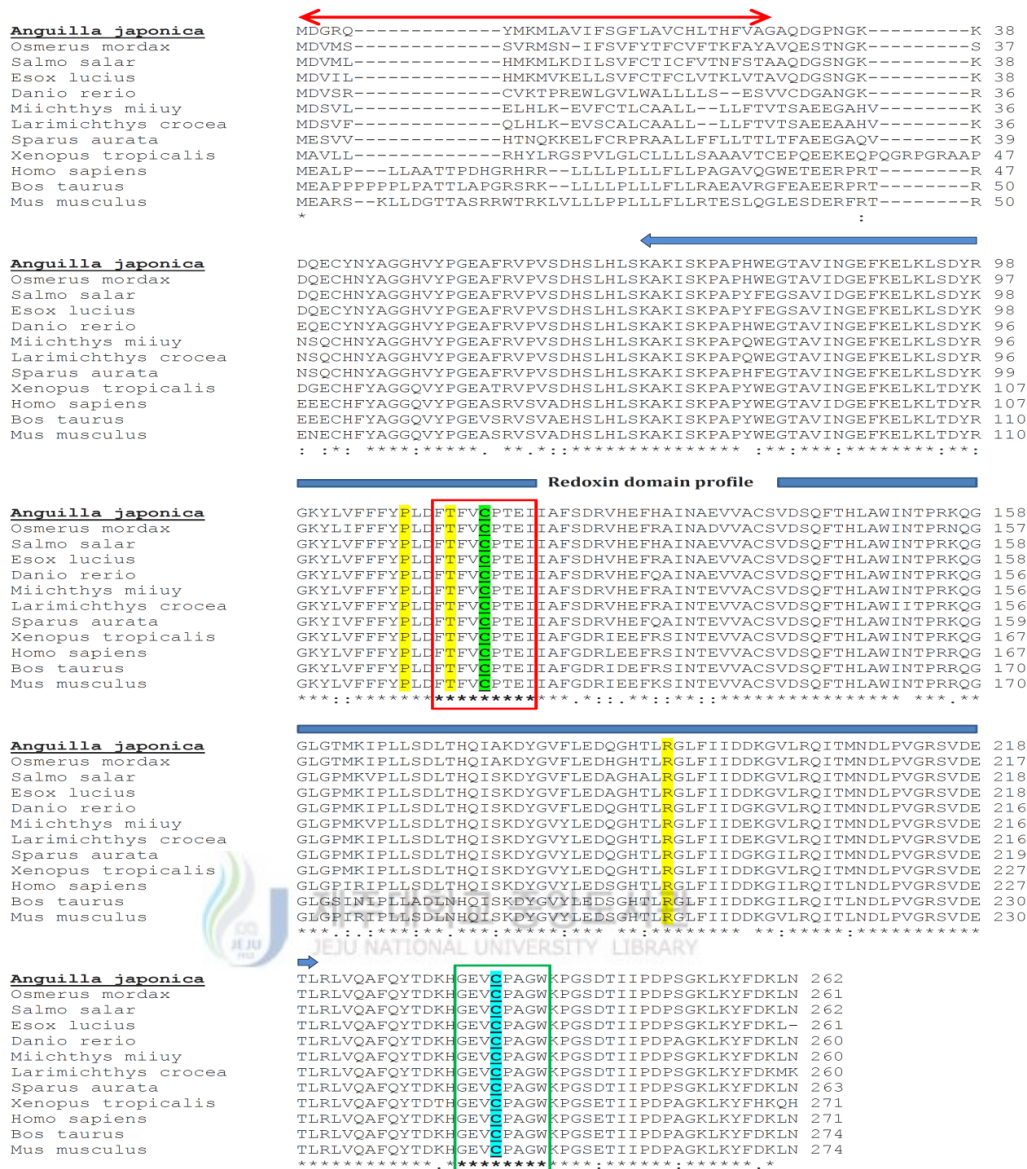


Fig. 15. Multiple sequence alignment of different vertebrate Prdx4s. Sequence alignments was obtained using the ClustalW method. Identical residues in all sequences are indicated by (*) under the column, conserved substitutions are indicated by (:), and semi-conserved substitutions are indicated by (.). Deletions are indicated by dashes. The redoxin domain profile is indicated by blue color double headed arrow. N-Terminus catalytic active site (¹¹¹FTFVCPTET¹²⁰) and C-terminus active site (²³³GEVCPAGW²⁴⁰) are boxed with red and green color respectively. N-Terminus signal sequence of AjPrdx4 is depicted by red color double headed arrow. Conserved peroxidatic cysteine residues C¹¹⁵ and conserved resolving cysteine residue C²³⁶ are highlighted with green and sky blue color respectively. Important conserved amino acids residues involve in the peroxidatic catalytic triad (P¹⁰⁸, T¹¹⁰ and R¹⁹¹) are shaded with blue.

3.2.2. Phylogenetic analysis

The phylogenetic tree undertaken in the present study evidenced three major clades corresponding to Prdx1-4 (typical 2-Cys Prdx subclass), Prdx5 (atypical 2-Cys Prdx subclass) and Prdx6 (1-Cys Prdx subclass) according to the present hierarchy of vertebrates (Fig. 16). As expected the AjPrdx4 was clustered with typical 2-Cys Prdx main clade, further positioned in Prdx4 sub clade with closest evolutionary proximity to Prdx4 from Rainbow smelt (*Osmerus mordax*) (Fig. 16). Therefore, these observations affirmed that AjPrdx4 has evolved from a common ancestor indicating that it is indeed an ortholog of vertebrate typical 2-Cys Prdx subgroup.



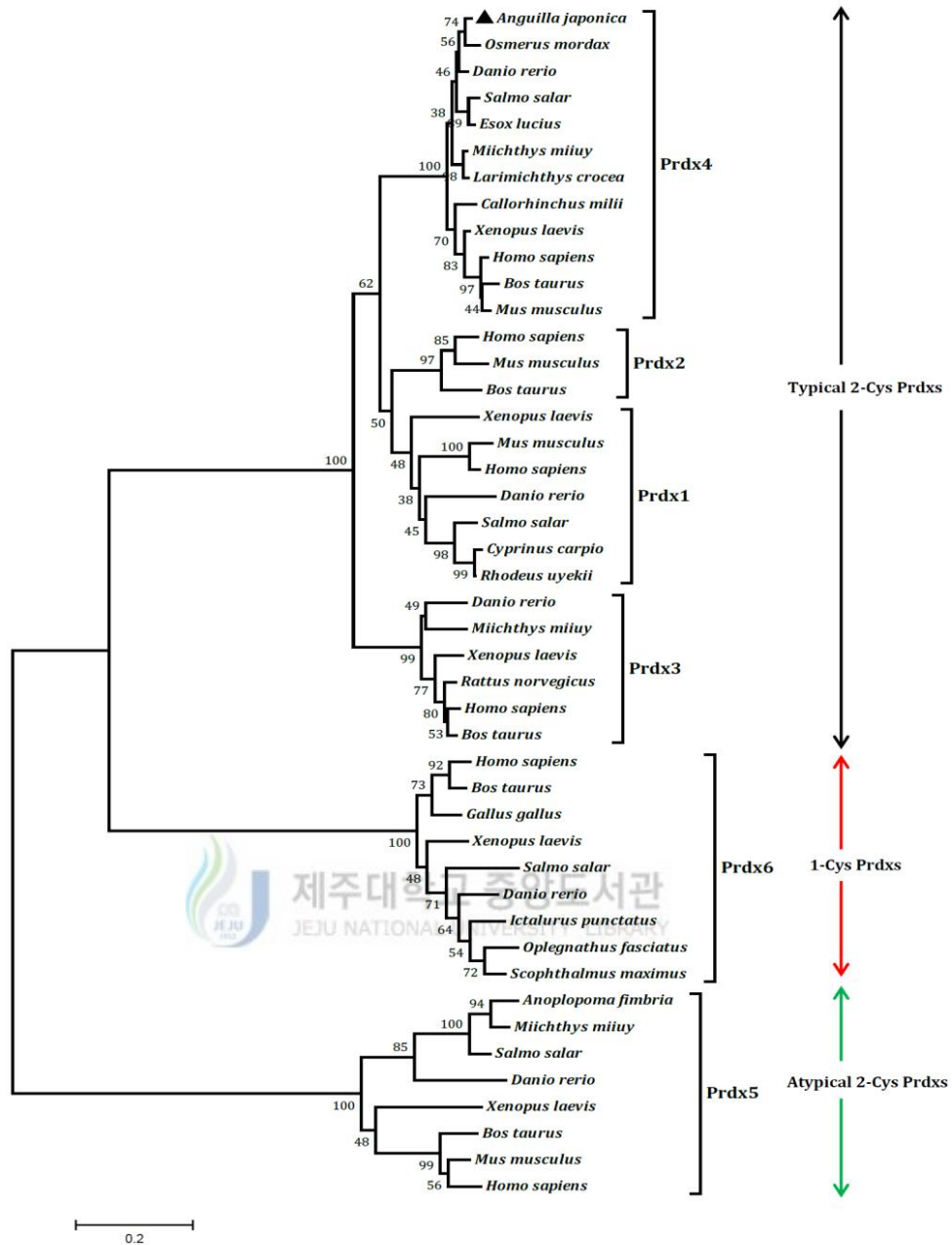


Fig. 16. Phylogenetic tree of known Prdxs from different species including the AjPrdx4. The tree was constructed based on multiple alignment of the overall sequences by neighbor-joining method. Bootstrap values are shown next to the branches based on 1000 replications.

3.2.3. Modeled tertiary structure of AjPrdx4

In order to correlate the function of AjPrdx4 with its structural properties, the 3D structure of AjPrdx4 was generated using ITASSER online server. Anticipated 3D modal of AjPrdx4 was accomplished using top 10 compatible templates structures

obtained from Research Collaboratory for Structural Bioinformatics (RCSB) protein data bank exhibited 22%- 68% identity with the query sequence. The best model was selected based on the C-score (confidence score), which estimates the quality of predicted models by I-TASSER. (Zhang, 2008). Moreover, the normalized Z-score values of the threading alignments exceeded 1, substantiating the higher degree of confidence of the predicted structure. The main body of the AjPrdx4 protein was consisted of seven core stranded β sheets flanked by nine α helices (Fig. 17A). Furthermore, two conserved N-terminus and C-terminus catalytic active site centers along with respective peroxidatic cysteine residue C¹¹⁵ and resolving cysteine residue C²³⁶ were identified in the generated modal of AjPrdx4 (Fig. 17A). Likewise, previously discovered Prdx structures, the conserved peroxidatic cysteine residue (C¹¹⁵) of AjPrdx4 was positioned in the first turn of 2nd α -helix in the redoxin domain profile (Fig. 17B) (Mu et al., 2013). Moreover C¹¹⁵ was surrounded by three highly conserved amino acid residues P¹⁰⁸, T¹¹⁰ and R¹⁹¹ which were believed to play significant role in facilitate the redox catalytic reaction. As depicted in Fig. 17B, the peroxidatic cysteine (C¹¹⁵) and resolving cysteine (C²³⁶) were positioned in opposite ends of the AjPrdx4 protein. Therefore this structural arrangement would be abolished the formation of intra molecular disulfide bonds between peroxidatic and resolving cysteine during the catalytic reaction of Prdx4. Further it might be attributed to the fact of formation of intermolecular disulfide bond between peroxidatic cysteine and resolving cysteine at the C terminus of the other subunit of Prdx4 during the catalytic reaction (Kawazu et al., 2008). Moreover it has been demonstrated that the formation of inter molecular disulfide bonds between separate molecules is a key feature of typical 2-Cys Prdx family. Altogether this findings affirms the correct orientation of the 3D globular arrangement of AjPrdx4 with respect to its functional properties

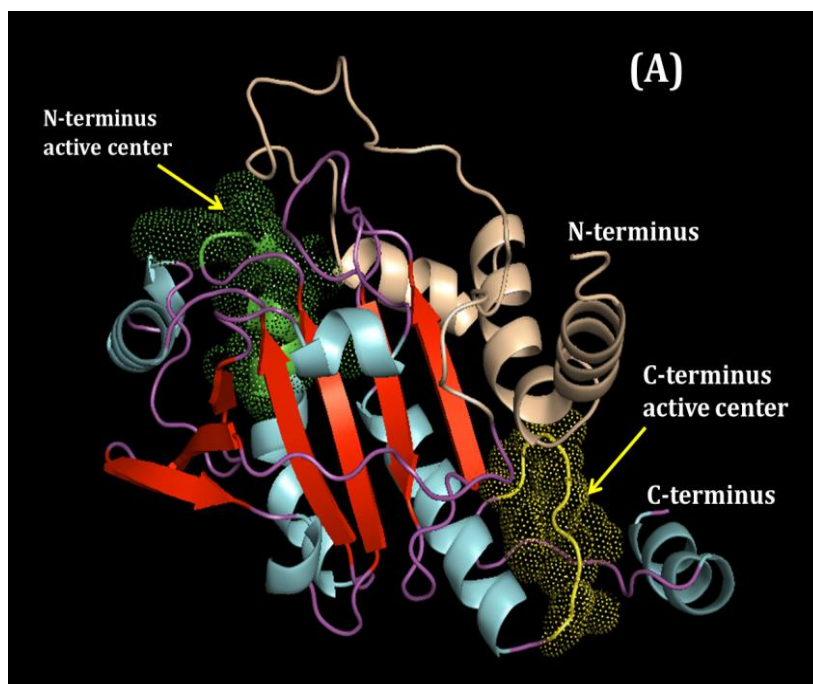


Fig. 17A. Computer simulation model generated for the AjPrdx4. (A) Tertiary structure elements belonging to the redoxin domain profile: (sky blue) α -helices, (Red) β -sheets. The N-terminus catalytic active center and C-terminus catalytic active center are represented with green and yellow dots respectively.

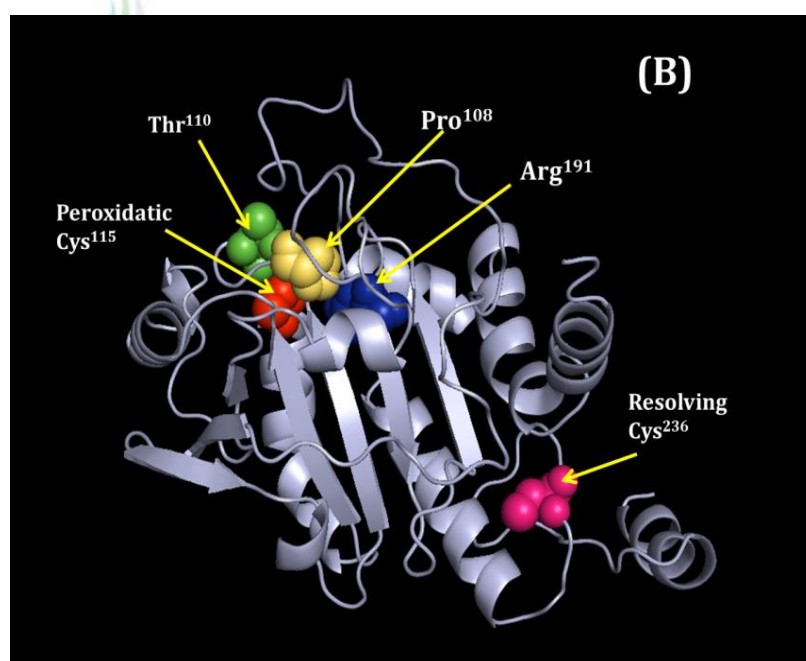


Fig. 17B. The 3D structure of AjPrdx4 with important conserved amino acid residues. The Conserved peroxidatic cysteine residues C^{115} and conserved resolving cysteine residue C^{236} are marked with red and pink color spheres respectively. The amino acid residues in peroxidatic catalytic triad, P^{108} , T^{110} and R^{191} are depicted using yellow, green and blue spheres respectively.

3.2.4. Tissue distribution analysis of *AjPrdx4*

The tissue specific expression level of *Anguilla japonica Prdx4* in healthy fish was detected by using qPCR. The expression varied among different tissues. Skin was used as a calibrator and defined its expression level as 1.000. As shown in Fig. 18, the *AjPrdx4* was ubiquitously expressed among all the tissues we tested, including liver, spleen, muscle, heart, skin, kidney, headkidney, gill, gonad and intestine. Highest expression of *AjPrdx4* was detected in heart followed by muscles and brain while liver, spleen, intestine, gill kidney head kidney showed low levels of *AjPrdx4* expression. Studies of the tissue specific distribution of miiuy croaker (*Miichthys miiuy*) demonstrated that *Prdx4* mRNA transcripts were predominantly expressed in spleen, intestine, and kidneys, whereas lowest levels were detected in eye liver, muscle (Ren et al., 2014). Moreover Jaume Pérez-Sánchez and group reported that gilthead sea bream (*Sparus aurata*) *Prdx4* was highly expressed in liver, and rest of the tissues showed very weak expression level (Perez-Sanchez et al., 2011). Studies of the tissue distribution of *Prdx4* in rats and humans showed that *Prdx4* mRNA is expressed in the digestive gland (liver) and reproductive organs (testis) at relatively high levels (Iuchi et al., 2009). Altogether, we suggested variation of transcriptional expression profiles of *Prdx4* in different fish may be due to expressional variability of different counterparts of *Prdx4* in different organs.

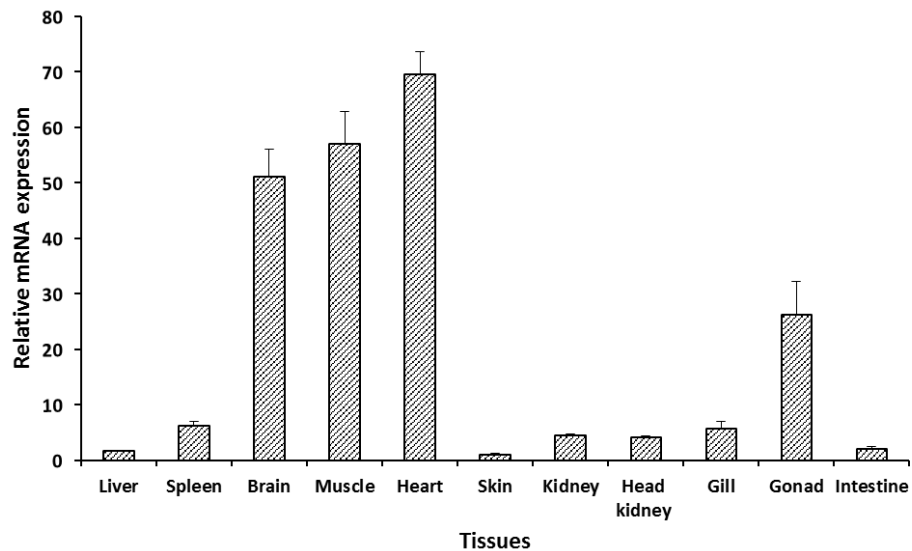


Fig. 18. Tissue specific expression analysis of *AjPrdx4* mRNA in healthy *Anguilla japonica* by qPCR. The mRNA expression level of each tissue is expressed relative to the mRNA expression in skin tissue. Each bar represents the standard error (SE) of triplicates (n = 5).

3.2.5. Regulation of *AjPrdx4* expression in response to pathogenic infection

In order to reveal the innate immune responses of *AjPrdx4*, its temporal mRNA expression profile was investigated under pathological conditions. Herein *E. tarda* a gram negative fish pathogen along with well characterized mitogens LPS and Poly I:C were used as stimulators. The Liver tissues were selected as candidate tissue for the examination, due to its significant role in innate immune defense in vertebrates. The mRNA expression level of *AjPrdx4* was quantified by qPCR using *AjEF-1a* as an internal control gene. As expected, *AjEF-1a* did not show any significant variation on this experiment under any of the provided condition affirming its suitability to be used as an internal reference.

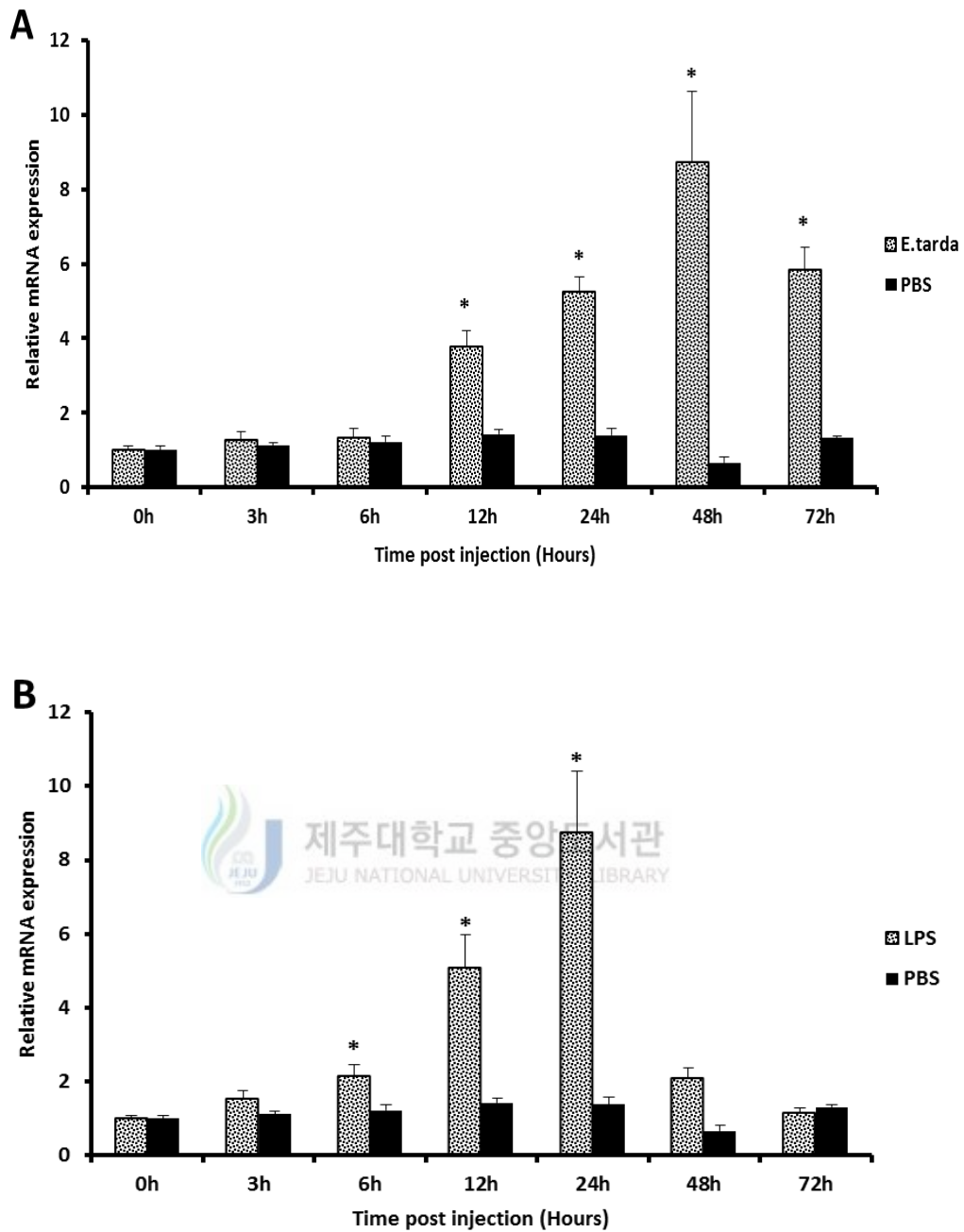


Fig. 19A,B. Relative mRNA expression pattern of *AjPrdx4* in liver after the stimulation with *Edwardsiella tarda* (A) and LPS (B). The expression analysis of *AjPrdx4* was determined by SYBR green quantitative real time PCR. Livak $2^{-\Delta\Delta CT}$ method was used to calculate relative expression levels using *Anguilla japonica EF-1a* as internal control gene. Each bar represents the standard error (SE) of five individual samples (n=5). Asterisk (*) represents the significant difference in expression against the un-injected control ($p < 0.05$).

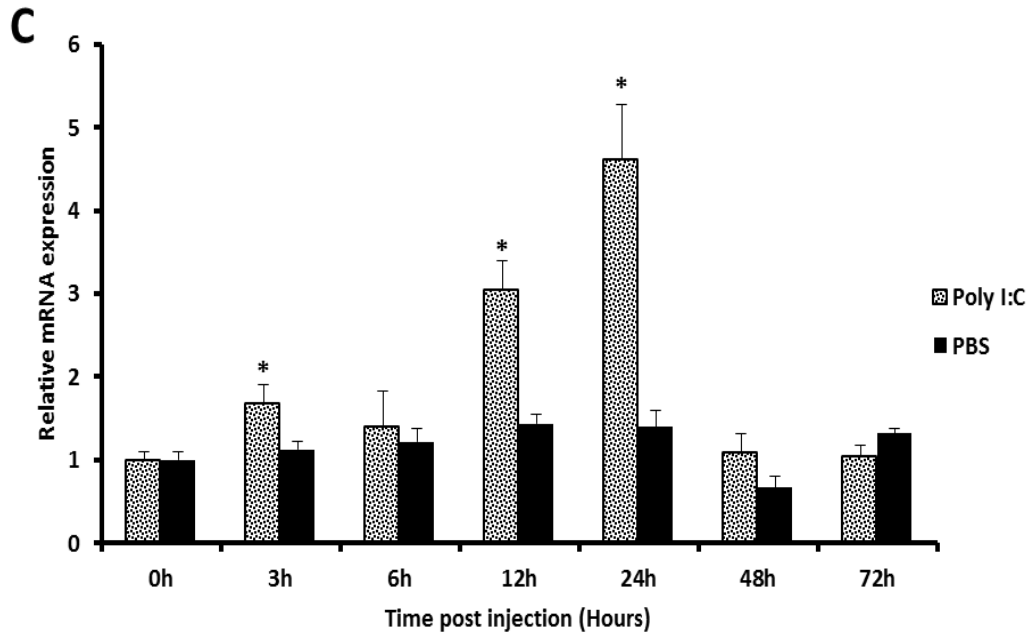


Fig. 19C. Relative mRNA expression pattern of *AjPrdx4* in liver after the stimulation with Poly I:C. The expression analysis of *AjPrdx4* was determined by SYBR green quantitative real time PCR. Livak $2^{-\Delta\Delta CT}$ method was used to calculate relative expression levels using *Anguilla japonica EF-1a* as internal control gene. Each bar represents the standard error (SE) of five individual samples (n=5). Asterisk (*) represents the significant difference in expression against the un-injected control ($P < 0.05$).

As shown in Fig. 19A, transcription up-regulation of *AjPrdx4* mRNA upon *E. tarda* showed highest induction fold at 48 h post injection (p.i) and amount of transcripts were gradually increased from 0 h to 48 h p.i. after reaching to the maximum level induction fold was reduced at 72 h p.i. Moreover significantly different induction folds of *AjPrdx4* mRNA transcripts were detected at 12 h, 24 h, 48 h p.i. after *E. tarda* injection compared to the un-injected control group. After the LPS stimulation, *AjPrdx4* mRNA transcripts were significantly up-regulated at 6 h, 12 h, 24 h p.i (Fig. 19B). Unlike with *E. tarda* stimulation, the maximum induction fold was reached at 24 h p.i and then induction fold was gradually reduced at the late phase of experiment (Fig. 19B) following LPS stimulation. Furthermore, *AjPrdx4* mRNA transcripts were gradually up-regulated from 6 h-24 h p.i. of Poly I:C injection and reached to maximum level,

there after expression of *AjPrdx4* transcripts were suddenly reduced at 48 h p.i (Fig. 19C). During the experiment of Poly I:C challenge, significant elevation of *AjPrdx4* mRNA transcripts were observed at 3 h , 12 h and 24 h p.i.

The *Prdxs* are known as antioxidant genes; however several immune responses of *Prdxs* upon pathological conditions have been documented (Yang et al., 2007). A previous study conducted in miiuy croaker (*Miichthys miiuy*), found that *Prdx4* expression was induced in liver by gram negative bacteria (*Vibrio anguillarum*) (Ren et al., 2014). Interestingly there was no significant inductions could be detected at early phase of the experiment and induction folds were quite lower compared to the control. Moreover, highest peak of the induction was detected at 48h p.i. of *V. anguillarum* injection as we obtained from our experiment (Fig. 19A). Furthermore several experiments revealed that the up-regulation of typical 2-Cys Prdx subgroup under bacterial (specially gram negative) infection, for example Jiong Chen and group found up-regulation of natural killer enhancing factor (NKFE) B also known as *Prdx2* upon *Aeromonas hydrophila* infection in liver tissues of *Plecoglossus altivelis* (Chen et al., 2009), as well as elevation of NKEF mRNA transcript under *E. tarda* infection of rockbreem head kidney tissues were investigated (Kim et al., 2011). Therefore, as a member of typical 2-Cys Prdx subgroup, there was a potential possibility to up-regulate the *AjPrdx4* mRNA transcripts under bacterial infection.

As depicted in Fig. 19A, induction fold of *AjPrdx4* in response to *E. tarda* treatment at early phase of the experiment was comparatively low or equal to the un-injected control group, and gradual up-regulation was observed until reach its maximum level. This observation can be attributed to the immune evasion mechanisms orchestrated by pathogenic organisms, especially bacteria against the host immune responses, including ROS production (Borjesson et al., 2005). According to the this

phenomena some bacterial pathogens like *E. tarda* can reduce the ROS production, whereby expression levels of antioxidant enzymes like *Prdx4* may not be highly expressed at the early phase of p.i of *E. tarda*. However subsequent up-regulation of *AjPrdx4* transcription may be triggered by other immune responses elicited by host cells to control the bacterial population.

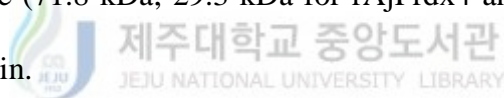
LPS is cell wall component of gram negative bacteria, which can be sensed by host through pattern recognition receptors, especially toll like receptor 4 (Kaihami et al., 2014). LPS is known to stimulate monocytes, macrophages, and neutrophils through the activation of transcription factors resulting in increased pro-inflammatory responses, associated with release of cytokines and other soluble mediators (Ostos et al., 2002). After the LPS injection, initial induction of *AjPrdx4* expression was detected at 6 h p.i and reached to maximum level at 24 h p.i in liver (Fig. 19B). Interestingly, at above mentioned points (initial significant induction of *AjPrdx4* expression and maximum induction level of *AjPrdx4*) were reached quite later upon the *E. tarda* treatment compared to LPS injection (Fig. 19A & B). This observation can be correlated with previously discussed immune evasion mechanism of *E. tarda*.

In this study, Poly I:C a viral double stranded RNA mimic was used to stimulate fish instead of virus, and it was significantly enhanced the transcription of *AjPrdx4* (Fig. 19C). The results reflected similar response as that LPS challenge with comparatively lower induction folds. Not only RNA viruses, the *Prdx4* transcription could be induced by DNA viruses. It has been shown up-regulation of *Prdx4* expression in several tissues from kuruma shrimp (*Marsupenaeus japonicas*) upon White spot syndrome virus (WSSV) showing the evidence that *Prdx4* might be involve in immune action against viruses (Chen et al., 2013). Furthermore, several reports have been illustrated that *Prdx4* is actively involved in preventing some bacterial and viral infection by

suppressing oxidative damage via various molecular mechanisms in mammals (Wong et al., 2000; Jamaluddin et al., 2010; Tavender and Bulleid, 2010; Kim et al., 2012). Collectively our finding suggested that the *AjPrdx4* evidently involved in the early innate immune responses orchestrated by pathogens or pathogen associated molecular patterns (PAMPs). However further experiments to be required for elucidate the detailed mechanism of immune responses of *AjPrdx4*.

3.2.6. Over expression of recombinant AjPrdx4 (rAjPrdx4)

To investigate the antioxidant activity, rAjPrdx4 fused with MBP was over-expressed in *E. coli* - BL21 (DE3) and purified using the pMAL purification system. The purified recombinant protein was analyzed by SDS-PAGE and a single band with a molecular mass of ~71.8 KDa was revealed (Fig. 20), which was in agreement with the theoretical size (71.8 kDa; 29.3 kDa for rAjPrdx4 and 42.5 kDa for MBP of the recombinant protein.



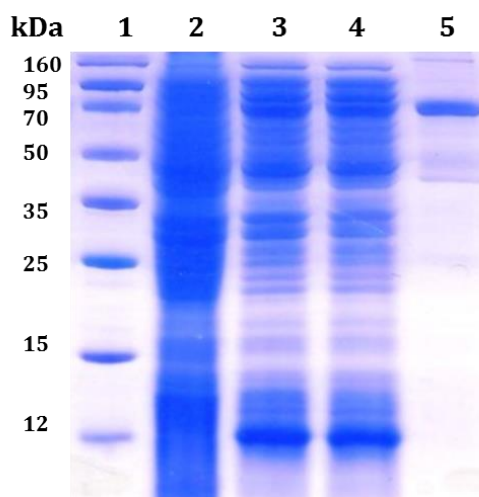


Fig. 20. SDS-PAGE analysis of the rAjPrdx4 fusion protein in *E. coli* BL21. Lanes 1, Protein size marker; lane 2, total cellular extract from *E. coli* BL21 carrying the rAjPrdx4-MBP expression vector prior to IPTG; lane 3, total protein of IPTG-induced *E. coli* (BL21) ; lane 4, soluble fraction; lane 5, purified recombinant fusion protein (rAjPrdx6-MBP) after IPTG induction.

3.2.7. Protective effects of recombinant rAjPrdx4 on cultured cells under oxidative stress

Purified rAjPrdx4-MBP was used to investigate the antioxidant activity of AjPrdx4 in vero (African green monkey kidney epithelial cells) under oxidative stress by MTT assay. The DTT was used as an electron donor to achieve the redox reaction between H₂O₂ and DTT to protect the bio molecules. In biology, the Prdxs were catalyzed the redox reaction with the help of thioredoxin or glutathione (Sutton et al., 2010). The average cell survival percentage results revealed that rAjPrdx4 has cell protection activity and reduce the mortality upon H₂O₂ oxidative stress. Even though there was not 100% protective effect of rAjPrdx4 on cell viability in any of the tested treatments except untreated cells (control), up to 80% cell survival was observed when the cells were treated with 25 mg/mL AjPrdx4 and 1 mM DTT in 100 mmol H₂O₂ exposed vero cells (Fig 21A, 21B and 21C). However, subsequent increases of rAjPrdx4 concentration resulted in stable cell protecting activity of rAjPrdx4 as

evidenced by graph (Fig. 21A). Furthermore, the initial protein concentrations (25 $\mu\text{g}/\text{mL}$) represent the optimal concentrations for cell protection at the given conditions. The control experiment with MBP did not show any significant cell protection activity. Furthermore, several antioxidant activities of recombinant Prdx including cell protection activity have been reported. Altogether our findings suggested that AjPrdx4 may express the active enzyme with typical antioxidant function in Japanese eel.

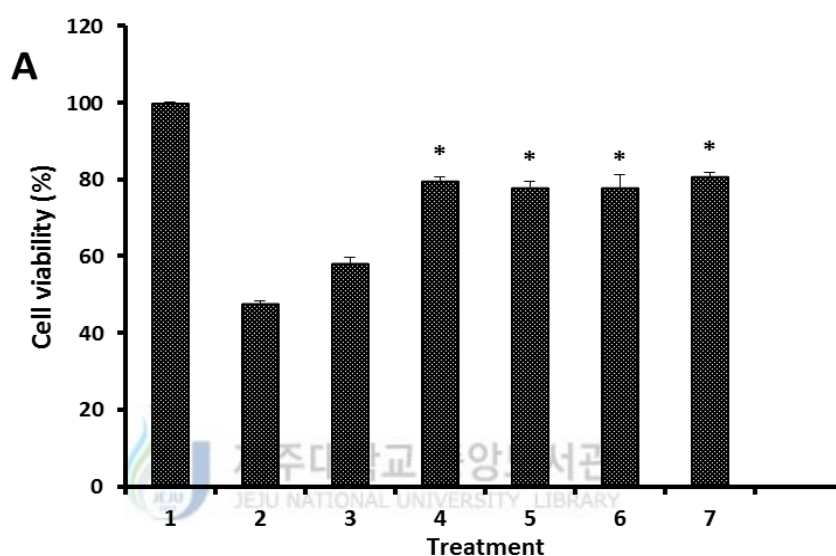


Fig. 21 (A) Effects of recombinant AjPrdx4 on cell growth and viability in 500 μM H_2O_2 exposed to vero cells. Cells were seeded at $2 \times 10^5/\text{mL}$ and pretreated with the different concentration combinations of rAjPdx6 for 30 min followed by treatment with 500 μM H_2O_2 for 24 h. Cell viability was determined by MTT assay. Treatments: (1) control cells; (2) cells treated with H_2O_2 (500 μM); (3) cells pretreated with MBP (100 $\mu\text{g}/\text{mL}$) and DTT (1 mM) followed by H_2O_2 (500 μM); (4) cells pretreated with rAjPrdx4 (25 $\mu\text{g}/\text{mL}$) and DTT (1 mM) followed by H_2O_2 (500 μM); (5) cells pretreated with rAjPrdx4 (50 $\mu\text{g}/\text{mL}$) and DTT (1 mM) followed by H_2O_2 (500 μM); (6) cells pretreated with rAjPrdx4 (75 $\mu\text{g}/\text{mL}$) and DTT (1 mM) followed by H_2O_2 (500 μM); (7) cells pretreated with rAjPrdx4 (120 $\mu\text{g}/\text{mL}$) and DTT (1 mM) followed by H_2O_2 (500 μM). Each bar represents the standard error (SE) of three individual samples ($n=3$). Asterisk (*) represents the significant difference in cell viability against the control ($p < 0.05$).

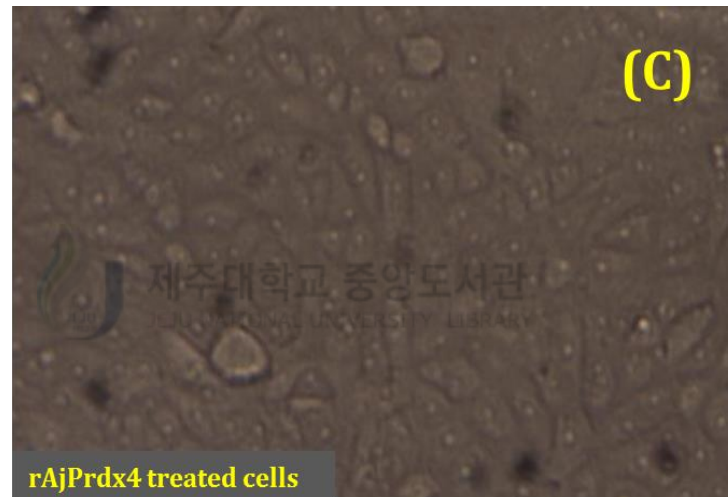
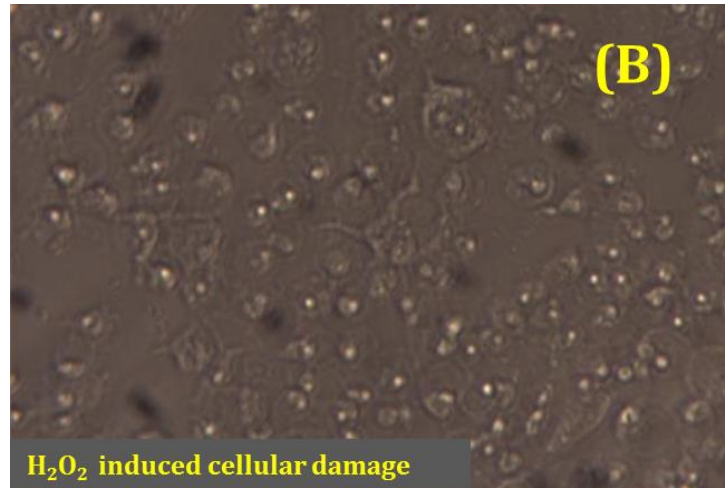


Fig. 21B,C. (B) Microscopic image of vero cells after the H₂O₂ (500 μM) treatment corresponding to treatment no 2 in Fig A; (C) Microscopic image of rAjPrdx4 (50μg/mL) pretreated vero cells with DTT (1 mM) followed by H₂O₂ (500 μM) corresponding to treatment no 4 in Fig 21A.

CONCLUSIONS

The cDNA sequences of Peroxiredoxin 4 (*AjPrdx4*) and Peroxiredoxin 6 (*AjPrdx6*) were identified from Japanese eel (*Anguilla japonica*). The deduced amino acid sequences of *AjPrdx4* and *AjPrdx6* exhibited prominent sequence similarity to their respective counterparts from teleosts. Furthermore *AjPrdx4* and *AjPrdx6* proteins harbored characteristic structural features and motifs of typical 2-Cys peroxiredoxin and 1-Cys peroxiredoxin subfamily respectively, implying those two proteins are indeed homologues of Peroxiredoxin superfamily. Moreover, the recombinant *AjPrdx4* and *AjPrdx6* proteins possessed *in vitro* protecting effects of H₂O₂ induced apoptosis in Vero cells showed that the purified *AjPrdx4* and *AjPrdx6* are functionally active, effectively eliminates H₂O₂. Ubiquitous *AjPrdx4* and *AjPrdx6* mRNA expressions were detected in all the tissues we tested. Furthermore, *AjPrdx4* and *AjPrdx6* mRNA transcripts were differently modulated upon three different immune stimulants, suggesting its potential role as an antioxidative enzyme in post immune responses at the protein level.

REFERENCES

- Alexopoulou, L., Holt, A.C., Medzhitov, R. and Flavell, R.A., 2001. Recognition of double-stranded RNA and activation of NF-kappaB by Toll-like receptor 3. *Nature* 413, 732-8.
- Aran, M., Ferrero, D.S., Pagano, E. and Wolosiuk, R.A., 2009. Typical 2-Cys peroxiredoxins-modulation by covalent transformations and noncovalent interactions. *FEBS J* 276, 2478-93.
- Borjesson, D.L., Kobayashi, S.D., Whitney, A.R., Voyich, J.M., Argue, C.M. and Deleo, F.R., 2005. Insights into pathogen immune evasion mechanisms: *Anaplasma phagocytophilum* fails to induce an apoptosis differentiation program in human neutrophils. *J Immunol* 174, 6364-72.
- Bryk, R., Lima, C.D., Erdjument-Bromage, H., Tempst, P. and Nathan, C., 2002. Metabolic enzymes of mycobacteria linked to antioxidant defense by a thioredoxin-like protein. *Science* 295, 1073-7.
- Chae, H.Z., Kang, S.W. and Rhee, S.G., 1999. Isoforms of mammalian peroxiredoxin that reduce peroxides in presence of thioredoxin. *Methods Enzymol* 300, 219-26.
- Chae, H.Z., Robison, K., Poole, L.B., Church, G., Storz, G. and Rhee, S.G., 1994. Cloning and sequencing of thiol-specific antioxidant from mammalian brain: alkyl hydroperoxide reductase and thiol-specific antioxidant define a large family of antioxidant enzymes. *Proc Natl Acad Sci U S A* 91, 7017-21.
- Chen, J., Wu, H.Q., Niu, H., Shi, Y.H. and Li, M.Y., 2009. Increased liver protein and mRNA expression of natural killer cell-enhancing factor B (NKEF-B) in ayu (*Plecoglossus altivelis*) after *Aeromonas hydrophila* infection. *Fish Shellfish Immunol* 26, 567-71.
- Chen, X.W., Kang, L.H., Ding, D., Liu, Q., Wang, J.X. and Kang, C.J., 2013. Characterization of a 2-Cys peroxiredoxin IV in *Marsupenaeus japonicus* (kuruma shrimp) and its role in the anti-viral immunity. *Fish Shellfish Immunol* 35, 1848-57.
- Choi, H.J., Kang, S.W., Yang, C.H., Rhee, S.G. and Ryu, S.E., 1998. Crystal structure of a novel human peroxidase enzyme at 2.0 Å resolution. *Nat Struct Biol* 5, 400-6.
- David, E., Tanguy, A. and Moraga, D., 2007. Peroxiredoxin 6 gene: a new physiological and genetic indicator of multiple environmental stress response in Pacific oyster *Crassostrea gigas*. *Aquat Toxicol* 84, 389-98.
- De Zoysa, M., Ryu, J.H., Chung, H.C., Kim, C.H., Nikapitiya, C., Oh, C., Kim, H., Saranya Revathy, K., Whang, I. and Lee, J., 2012. Molecular characterization, immune responses and DNA protection activity of rock bream (*Oplegnathus fasciatus*), peroxiredoxin 6 (Prx6). *Fish Shellfish Immunol* 33, 28-35.
- Ellis, H.R. and Poole, L.B., 1997a. Novel application of 7-chloro-4-nitrobenzo-2-oxa-1,3-diazole to identify cysteine sulfenic acid in the AhpC component of alkyl hydroperoxide reductase. *Biochemistry* 36, 15013-8.
- Ellis, H.R. and Poole, L.B., 1997b. Roles for the two cysteine residues of AhpC in catalysis of peroxide reduction by alkyl hydroperoxide reductase from *Salmonella typhimurium*. *Biochemistry* 36, 13349-56.
- Elofsson, A. and von Heijne, G., 2007. Membrane protein structure: prediction versus reality. *Annu Rev Biochem* 76, 125-40.
- Fujii, T., Fujii, J. and Taniguchi, N., 2001. Augmented expression of peroxiredoxin VI in rat lung and kidney after birth implies an antioxidative role. *Eur J Biochem* 268, 218-25.
- Furchgott, R.F., 1995. A research trail over half a century. *Annu Rev Pharmacol Toxicol* 35, 1-27.
- Gallagher, B.M. and Phelan, S.A., 2007. Investigating transcriptional regulation of Prdx6 in mouse liver cells. *Free Radic Biol Med* 42, 1270-7.
- Giguere, P., Turcotte, M.E., Hamelin, E., Parent, A., Brisson, J., Laroche, G., Labrecque, P., Dupuis, G. and Parent, J.L., 2007. Peroxiredoxin-4 interacts with and regulates the thromboxane A(2) receptor. *FEBS Lett* 581, 3863-8.

- Hamza, A., 2002. Homology modeling and docking mechanism of the mercaptosuccinate and methotrexate to *P. falciparum* 1-Cys peroxiredoxin: a preliminary molecular study. *J Biomol Struct Dyn* 20, 7-20.
- Han, J.Y., Song, K.D., Shin, J.H., Han, B.K., Park, T.S., Park, H.J., Kim, J.K., Lillehoj, H.S., Lim, J.M. and Kim, H., 2005. Identification and characterization of the peroxiredoxin gene family in chickens. *Poult Sci* 84, 1432-8.
- Haslekas, C., Viken, M.K., Grini, P.E., Nygaard, V., Nordgard, S.H., Meza, T.J. and Aalen, R.B., 2003. Seed 1-cysteine peroxiredoxin antioxidants are not involved in dormancy, but contribute to inhibition of germination during stress. *Plant Physiol* 133, 1148-57.
- Hofmann, B., Hecht, H.J. and Flohe, L., 2002. Peroxiredoxins. *Biol Chem* 383, 347-64.
- Iuchi, Y., Okada, F., Tsunoda, S., Kibe, N., Shirasawa, N., Ikawa, M., Okabe, M., Ikeda, Y. and Fujii, J., 2009. Peroxiredoxin 4 knockout results in elevated spermatogenic cell death via oxidative stress. *Biochem J* 419, 149-58.
- Jamaluddin, M., Wiktorowicz, J.E., Soman, K.V., Boldogh, I., Forbus, J.D., Spratt, H., Garofalo, R.P. and Brasier, A.R., 2010. Role of peroxiredoxin 1 and peroxiredoxin 4 in protection of respiratory syncytial virus-induced cysteinyl oxidation of nuclear cytoskeletal proteins. *J Virol* 84, 9533-45.
- Kaihami, G.H., Almeida, J.R., Santos, S.S., Netto, L.E., Almeida, S.R. and Baldini, R.L., 2014. Involvement of a 1-cys peroxiredoxin in bacterial virulence. *PLoS Pathog* 10, e1004442.
- Kang, S.W., Baines, I.C. and Rhee, S.G., 1998. Characterization of a mammalian peroxiredoxin that contains one conserved cysteine. *J Biol Chem* 273, 6303-11.
- Kang, S.W., Rhee, S.G., Chang, T.S., Jeong, W. and Choi, M.H., 2005. 2-Cys peroxiredoxin function in intracellular signal transduction: therapeutic implications. *Trends Mol Med* 11, 571-8.
- Kawazu, S., Komaki-Yasuda, K., Oku, H. and Kano, S., 2008. Peroxiredoxins in malaria parasites: parasitologic aspects. *Parasitol Int* 57, 1-7.
- Kim, J.W., Choi, H.S., Kwon, M.G., Park, M.A., Hwang, J.Y., Kim, D.H. and Park, C.I., 2011. Molecular identification and expression analysis of a natural killer cell enhancing factor (NKEF) from rock bream *Oplegnathus fasciatus* and the biological activity of its recombinant protein. *Results Immunol* 1, 45-52.
- Kim, T.H., Song, J., Alcantara Llaguno, S.R., Murnan, E., Liyanarachchi, S., Palanichamy, K., Yi, J.Y., Viapiano, M.S., Nakano, I., Yoon, S.O., Wu, H., Parada, L.F. and Kwon, C.H., 2012. Suppression of peroxiredoxin 4 in glioblastoma cells increases apoptosis and reduces tumor growth. *PLoS One* 7, e42818.
- Leavey, P.J., Gonzalez-Aller, C., Thurman, G., Kleinberg, M., Rinckel, L., Ambruso, D.W., Freeman, S., Kuypers, F.A. and Ambruso, D.R., 2002. A 29-kDa protein associated with p67phox expresses both peroxiredoxin and phospholipase A2 activity and enhances superoxide anion production by a cell-free system of NADPH oxidase activity. *J Biol Chem* 277, 45181-7.
- Lehtonen, S.T., Svensk, A.M., Soini, Y., Paakko, P., Hirvikoski, P., Kang, S.W., Saily, M. and Kinnula, V.L., 2004. Peroxiredoxins, a novel protein family in lung cancer. *Int J Cancer* 111, 514-21.
- Ling, S.H., Wang, X.H., Xie, L., Lim, T.M. and Leung, K.Y., 2000. Use of green fluorescent protein (GFP) to study the invasion pathways of *Edwardsiella tarda* in vivo and in vitro fish models. *Microbiology* 146 (Pt 1), 7-19.
- Livak, K.J. and Schmittgen, T.D., 2001. Analysis of relative gene expression data using real-time quantitative PCR and the 2(-Delta Delta C(T)) Method. *Methods* 25, 402-8.
- Loo, G.H. and Schuller, K.A., 2010. Cloning and functional characterization of a peroxiredoxin 4 from yellowtail kingfish (*Seriola lalandi*). *Comp Biochem Physiol B Biochem Mol Biol* 156, 244-53.
- Loumaye, E., Andersen, A.C., Clippe, A., Degand, H., Dubuisson, M., Zal, F., Morsomme, P., Rees, J.F. and Knoops, B., 2008. Cloning and characterization of *Arenicola marina* peroxiredoxin 6, an annelid two-cysteine peroxiredoxin highly homologous to mammalian one-cysteine peroxiredoxins. *Free Radic Biol Med* 45, 482-93.

- Manevich, Y. and Fisher, A.B., 2005. Peroxiredoxin 6, a 1-Cys peroxiredoxin, functions in antioxidant defense and lung phospholipid metabolism. *Free Radic Biol Med* 38, 1422-32.
- Matsumoto, A., Okado, A., Fujii, T., Fujii, J., Egashira, M., Niikawa, N. and Taniguchi, N., 1999. Cloning of the peroxiredoxin gene family in rats and characterization of the fourth member. *FEBS Lett* 443, 246-50.
- Mosmann, T., 1983. Rapid colorimetric assay for cellular growth and survival: application to proliferation and cytotoxicity assays. *J Immunol Methods* 65, 55-63.
- Mu, C., Zhao, J., Wang, L., Song, L., Zhang, H., Li, C., Qiu, L. and Gai, Y., 2009. Molecular cloning and characterization of peroxiredoxin 6 from Chinese mitten crab *Eriocheir sinensis*. *Fish Shellfish Immunol* 26, 821-7.
- Mu, Y., Lian, F.M., Teng, Y.B., Ao, J., Jiang, Y.L., He, Y.X., Chen, Y., Zhou, C.Z. and Chen, X., 2013. The N-terminal beta-sheet of peroxiredoxin 4 in the large yellow croaker *Pseudosciaena crocea* is involved in its biological functions. *PLoS One* 8, e57061.
- Nikapitiya, C., De Zoysa, M., Whang, I., Kim, C.G., Lee, Y.H., Kim, S.J. and Lee, J., 2009. Molecular cloning, characterization and expression analysis of peroxiredoxin 6 from disk abalone *Haliotis discus discus* and the antioxidant activity of its recombinant protein. *Fish Shellfish Immunol* 27, 239-49.
- Nogoceke, E., Gommel, D.U., Kiess, M., Kalisz, H.M. and Flohe, L., 1997. A unique cascade of oxidoreductases catalyses trypanothione-mediated peroxide metabolism in *Crithidia fasciculata*. *Biol Chem* 378, 827-36.
- Nordberg, J. and Arner, E.S., 2001. Reactive oxygen species, antioxidants, and the mammalian thioredoxin system. *Free Radic Biol Med* 31, 1287-312.
- Okonechnikov, K., Golosova, O., Fursov, M. and team, U., 2012. Unipro UGENE: a unified bioinformatics toolkit. *Bioinformatics* 28, 1166-7.
- Ostos, M.A., Recalde, D., Zakin, M.M. and Scott-Algara, D., 2002. Implication of natural killer T cells in atherosclerosis development during a LPS-induced chronic inflammation. *FEBS Lett* 519, 23-9.
- Palande, K., Roovers, O., Gits, J., Verwijmeren, C., Iuchi, Y., Fujii, J., Neel, B.G., Karisch, R., Tavernier, J. and Touw, I.P., 2011. Peroxiredoxin-controlled G-CSF signalling at the endoplasmic reticulum-early endosome interface. *J Cell Sci* 124, 3695-705.
- Palmer, R.M., Ferrige, A.G. and Moncada, S., 1987. Nitric oxide release accounts for the biological activity of endothelium-derived relaxing factor. *Nature* 327, 524-6.
- Park, H., Ahn, I.Y., Kim, H., Cheon, J. and Kim, M., 2008. Analysis of ESTs and expression of two peroxiredoxins in the thermally stressed Antarctic bivalve *Laternula elliptica*. *Fish Shellfish Immunol* 25, 550-9.
- Perez-Sanchez, J., Bermejo-Nogales, A., Calduch-Giner, J.A., Kaushik, S. and Sitja-Bobadilla, A., 2011. Molecular characterization and expression analysis of six peroxiredoxin paralogous genes in gilthead sea bream (*Sparus aurata*): insights from fish exposed to dietary, pathogen and confinement stressors. *Fish Shellfish Immunol* 31, 294-302.
- Peshenko, I.V. and Shichi, H., 2001. Oxidation of active center cysteine of bovine 1-Cys peroxiredoxin to the cysteine sulfenic acid form by peroxide and peroxyxynitrite. *Free Radic Biol Med* 31, 292-303.
- Poole, L.B., Reynolds, C.M., Wood, Z.A., Karplus, P.A., Ellis, H.R. and Li Calzi, M., 2000. AhpF and other NADH:peroxiredoxin oxidoreductases, homologues of low Mr thioredoxin reductase. *Eur J Biochem* 267, 6126-33.
- Ren, L., Sun, Y., Wang, R. and Xu, T., 2014. Gene structure, immune response and evolution: comparative analysis of three 2-Cys peroxiredoxin members of miiuy croaker, *Miichthys miiuy*. *Fish Shellfish Immunol* 36, 409-16.
- Ren, L., Xu, T., Wang, R. and Sun, Y., 2013. Miiuy croaker (*Miichthys miiuy*) Peroxiredoxin2: molecular characterization, genomic structure and immune response against bacterial infection. *Fish Shellfish Immunol* 34, 556-63.

- Reshi, M.L., Su, Y.C. and Hong, J.R., 2014. RNA Viruses: ROS-Mediated Cell Death. *Int J Cell Biol* 2014, 467452.
- Rhee, S.G., Chae, H.Z. and Kim, K., 2005. Peroxiredoxins: a historical overview and speculative preview of novel mechanisms and emerging concepts in cell signaling. *Free Radic Biol Med* 38, 1543-52.
- Rhee, S.G., Kang, S.W., Chang, T.S., Jeong, W. and Kim, K., 2001. Peroxiredoxin, a novel family of peroxidases. *IUBMB Life* 52, 35-41.
- Rosen, H., Orman, J., Rakita, R.M., Michel, B.R. and VanDevanter, D.R., 1990. Loss of DNA-membrane interactions and cessation of DNA synthesis in myeloperoxidase-treated *Escherichia coli*. *Proc Natl Acad Sci U S A* 87, 10048-52.
- Rudneva, I., 1999. Antioxidant system of Black Sea animals in early development. *Comp Biochem Physiol C Pharmacol Toxicol Endocrinol* 122, 265-71.
- Singh, A.K. and Shichi, H., 1998. A novel glutathione peroxidase in bovine eye. Sequence analysis, mRNA level, and translation. *J Biol Chem* 273, 26171-8.
- Stadtman, E.R. and Levine, R.L., 2000. Protein oxidation. *Ann N Y Acad Sci* 899, 191-208.
- Stuhlmeier, K.M., Kao, J.J., Wallbrandt, P., Lindberg, M., Hammarstrom, B., Broell, H. and Paigen, B., 2003. Antioxidant protein 2 prevents methemoglobin formation in erythrocyte hemolysates. *Eur J Biochem* 270, 334-41.
- Sutton, D.L., Loo, G.H., Menz, R.I. and Schuller, K.A., 2010. Cloning and functional characterization of a typical 2-Cys peroxiredoxin from southern bluefin tuna (*Thunnus maccoyii*). *Comp Biochem Physiol B Biochem Mol Biol* 156, 97-106.
- Tavender, T.J. and Bulleid, N.J., 2010. Peroxiredoxin IV protects cells from oxidative stress by removing H₂O₂ produced during disulphide formation. *J Cell Sci* 123, 2672-9.
- Thomas, E.L., Lehrer, R.I. and Rest, R.F., 1988. Human neutrophil antimicrobial activity. *Rev Infect Dis* 10 Suppl 2, S450-6.
- Wong, C.M., Chun, A.C., Kok, K.H., Zhou, Y., Fung, P.C., Kung, H.F., Jeang, K.T. and Jin, D.Y., 2000. Characterization of human and mouse peroxiredoxin IV: evidence for inhibition by Prx-IV of epidermal growth factor- and p53-induced reactive oxygen species. *Antioxid Redox Signal* 2, 507-18.
- Wood, Z.A., Schroder, E., Robin Harris, J. and Poole, L.B., 2003. Structure, mechanism and regulation of peroxiredoxins. *Trends Biochem Sci* 28, 32-40.
- Yang, C.S., Lee, D.S., Song, C.H., An, S.J., Li, S., Kim, J.M., Kim, C.S., Yoo, D.G., Jeon, B.H., Yang, H.Y., Lee, T.H., Lee, Z.W., El-Benna, J., Yu, D.Y. and Jo, E.K., 2007. Roles of peroxiredoxin II in the regulation of proinflammatory responses to LPS and protection against endotoxin-induced lethal shock. *J Exp Med* 204, 583-94.
- Yang, D., Song, Y., Wang, X., Sun, J., Ben, Y., An, X., Tong, L., Bi, J., Wang, X. and Bai, C., 2011. Deletion of peroxiredoxin 6 potentiates lipopolysaccharide-induced acute lung injury in mice. *Crit Care Med* 39, 756-64.
- Yla-Herttuala, S., 1999. Oxidized LDL and atherogenesis. *Ann N Y Acad Sci* 874, 134-7.
- Zhang, Q., Huang, J., Li, F., Liu, S., Liu, Q., Wei, J., Liang, G. and Xiang, J., 2014. Molecular characterization, immune response against white spot syndrome virus infection of peroxiredoxin 4 in *Fenneropenaeus chinensis* and its antioxidant activity. *Fish Shellfish Immunol* 37, 38-45.
- Zhang, Y., 2008. I-TASSER server for protein 3D structure prediction. *BMC Bioinformatics* 9, 40.
- Zheng, W.J., Hu, Y.H., Zhang, M. and Sun, L., 2010. Analysis of the expression and antioxidative property of a peroxiredoxin 6 from *Scophthalmus maximus*. *Fish Shellfish Immunol* 29, 305-11.

ACKNOWLEDGEMENT

Foremost, I would like to express my sincere gratitude to my supervisor Prof. Jehee Lee for the continuous support of my M.Sc study and research, for his patience, motivation, enthusiasm, and immense knowledge. His guidance helped me in all the time of research and writing of this thesis. Without his guidance as a great mentor, this work would not have been possible, and I certainly wouldn't be here. I would also like to express my deepest gratitude to Dr. Bong Soo Lim and Dr. Hyung-Bok Jeong for their excellent guidance, caring, patience, and providing me with an excellent atmosphere for doing research.

Secondly, I lend my sincere thanks to Dr. Seong il Kang, Dr. Ilson Whang, Dr. Qiang Wan and Dr. Changnam Jin for taking their valuable time and providing great input into this work. Besides my advisor, I would like to thank my thesis director Prof. Choon Bok Song for his encouragement, insightful comments, and hard questions.

I am also so thankful to my Korean colleagues: Yucheol Kim, Sukkyoung Lee, Seongdo Lee, Hyowon Kim, Minyoung Oh, Jaeyoung Choi, Eunyoung Jo, Jiyeon Ko, Ma Jeong In and Sunhye Kang for their continuous support and encouragement. In particular, I am grateful to my dear past and present colleagues: Anushka elvitigala, Chaminda Lakmal, Dr. Kalpa Samarakoon, Dr. Niroshana Wickramaarachchi, Sanjaya Bathige, Dr. Navaneethaiyer Umasuthan, Gelshan Imarshana, Viraj Udayantha, Lalinka Herath, Handun Eranga, Thulasi, Prasad Tharanga, Dilshara Matharage, Prathibhani, Hamsanandini, Mothi, Susara and Buddhi for their invaluable help and encouragement during my research and life in Korea.

Finally, I must express my very profound gratitude to my parents for providing me with unfailing support and continuous encouragement throughout my years of study

and through the process of researching and writing this thesis. This accomplishment would not have been possible without them. Thank you.

